Pure & Appl. Chem., Vol.55, No.6, pp.943-976, 1983.
Printed in Great Britain.

0033-4545/83/060943-34$03.00/0
Pergamon Press Ltd.

INTERNATIONAL UNION OF PURE AND APPLIED CHEMISTRY

MACROMOLECULAR DIVISION

COMMISSION ON POLYMER CHARACTERIZATION AND PROPERTIES

WORKING PARTY ON STRUCTURE AND PROPERTIES OF COMMERCIAL POLYMERS*

A COLLABORATIVE STUDY ON THE RELATION BETWEEN FILM BLOWING PERFORMANCE AND RHEOLOGICAL PROPERTIES OF TWO LOW-DENSITY AND TWO HIGH-DENSITY POLYETHYLENE SAMPLES

Prepared for publication by

H. H. WINTER

Department of Chemical Engineering,
University of Massachusetts, Amherst, USA

*Membership of the Working Party engaged on this programme during 1979-81 was principally as follows:

Chairman: P. L. CLEGG (UK); *Secretary:* M. E. CARREGA (France); *Members:* G. AJROLDI (Italy); J. M. CANN (UK); J. C. CHAUFFOUREAUX (Belgium); F. N. COGSWELL (UK); D. CONSTANTIN (France); H. COSTER (Netherlands); M. FLEISSNER (FRG); C. GERTH (FRG); A. GHIJSELS (Netherlands); G. GOLDBACH (FRG); P. B. KEATING (Belgium); A. S. LODGE (USA); J. MEISSNER (Switzerland); H. MÜNSTEDT (FRG); A. PLOCHOCKI (Poland); G. SCHOUKENS (Belgium); J. SEFERIS (USA); E. SCHUT (Netherlands); A. J. de VRIES (France); J. L. S. WALES (Netherlands); J. L. WHITE (USA); H. H. WINTER (USA); J. YOUNG (Netherlands).

A COLLABORATIVE STUDY ON THE RELATION BETWEEN FILM BLOWING PERFORMANCE AND RHEOLOGICAL PROPERTIES OF TWO LOW-DENSITY AND TWO HIGH-DENSITY POLYETHYLENE SAMPLES

Abstract - Two pairs of polyethylenes (HDPE, LDPE) were studied in fourteen laboratories. The experiments concentrated on film blowing and on laboratory tests. Laboratory tests were performed on crystallization from the melt, shear viscosity (steady and time dependent), storage modulus, loss modulus, relaxation modulus, entrance pressure correction, melt flow index, extrudate swell, uniaxial extensional creep, recovery after uniaxial extension, and tensile test on extrudate. The samples were chosen so that their film blowing behavior is significantly different, but the behavior in shear flow is similar. The goal of the study is to select laboratory tests which are as sensitive to material differences as the actual film blowing process is. A correlation of such sensitive laboratory tests with film blowing will be a basis for predicting the technological behavior of commercial polymers. -The two LDPE samples were polymerized in different batches. The two HDPE samples were prepared from the same powder lot and differ by the kind of processing aid (zinc or calcium stearate) which was added before granulating. -The crystallization behavior was found to be different within each pair or about the same, depending on the participating laboratories; no satisfactory agreement could be achieved. -The most sensitive rheological tests were found to involve extensional flow. Other sensitive rheological tests were in shear when dominated by long time constants (zero viscosity, stress relaxation). For both pairs, the sample with the lower extensional viscosity can be extended the most in the tensile test and can be blown into the thinnest film. -Crystallization and extensional rheology seem to be the two most important areas in laboratory testing, as used for distinguishing between polyethylene film blowing materials.

1. INTRODUCTION, PARTICIPATING LABORATORIES

In a previous IUPAC program (1) three similar low density polyethylene samples were blown into a film and were subjected to extensive rheological experiments. There were differences in the technological behavior (maximum film drawn down, s_f/s_0, and optical properties). However, the three samples had practically indistinguishable behavior in

a) the melt flow index at 190°C,
b) the linear viscoelastic range,
c) the viscosity function.

Laboratory tests which showed differences were on the maximum normal stress growth in shear flow, extensional flow, melt flow index at low temperature. The sample with the lowest tensile stress in uniaxial extension could be drawn into the thinnest film. In a recent publication, differences in shear creep at long times and low shear rates were found by Agarwal and Plazek (2). Small differences in isothermal crystallization were found by members of the working party, later confirmed by Magill and Peddada (3).

The following film blowing study has been undertaken to substantiate the correlation between extensional behavior and film blowing. This required an extension of the work to other polyethylene types: two new pairs of samples were selected in such a way that only small differences appeared in the shear viscosity function at high shear rate, but pronounced differences appeared in the film blowing behavior. These samples were tested in crystallization, in rheological experiments, and in the film blowing process. The measurements on the processing behavior have been approved so as to be more comparable in precision and reproducibility with melt rheology studies; for example, the critical drawdown condition (extensibility at break) was determined by means of a continuously variable drawdown speed.

Manufacturers of film grade polyethylenes evaluate the processing behavior in the actual film blowing process itself. The minimum amount of material for one test is about 50 kg. Thus a valuable result of this program would be to find a (small sample) rheological test for the prediction of the actual film blowing behavior.

This report describes the contributions of several laboratories. The name of the laboratories will be abbreviated in the text:

BASF AG, Ludwigshafen, West Germany	(BASF)
CdF CHIMIE, Mazingarbe, France	(CdF)
Centraal Laboratorium TNO, Delft, Netherlands	(TNO)
Chem. Werke Huls AG, Marl, West Germany	(CWH)
ETH Zurich, Techn.-Chem. Laboratorium, Switzerland	(ETH)
Hoechst AG, Frankfurt/Main, West Germany	(Hoechst)
ICI Plastics Division, Welwyn Garden City, England	(ICI)
Instytut Chemii Przemyslowej, Warschau, Poland	(ICHP)
Koninklijke Shell Laboratorium, Amsterdam, Netherlands	(Shell)
Montedison Centro Ricerche, Bollate and Ferrara, Italy	(ME)
Rhone-Poulenc Industries, Aubervilliers, France	(RP)
Solvay & Cie, Laboratoire Central, Bruxelles, Belgium	(Solvay)
U. Stuttgart, Inst. f. Kunststofftechnologie, W. Germany	(IKT)
U. Massachusetts, Amherst, Chemical Engr., USA	(UMass)

2. MATERIALS

The polymers are one pair of low density polyethylene (samples I and II) supplied by BASF, and one pair of high density polyethylene (samples C and Z) supplied by Hoechst.
No attempt will be made to give a detailed model of the film blowing process. Process studies can be found in references 4-13.

LDPE samples I and II

Both samples are similar to the commercial film blowing material Lupolen 3020 K of BASF. The samples are highly stabilized. They were polymerized in separate batches. Sample I seems to have a higher average molecular weight. It contains a larger fraction of molecules with large molecular weight (Fig. 1). The number averages molecular weight, M_n is about the same for the two samples (25,000-26,000), but the weight average molecular weight, M_w is much higher for sample I (169,000 versus 130,000) (CdF).

Branching of the two samples has been measured by a combined infrared spectroscopy/^{13}C nuclear magnetic resonance method (14-16). The two polyethylenes have similar branching, see Table 1.

HDPE samples C and Z

Both samples are similar to the commercial film blowing material Hostalen GM 9255 F of Hoechst. This is a high molecular weight material for manufacturing high impact films with paper-like character. The two samples were prepared from the same powder lot and differ by the kind of processing aid which was added before granulating. Sample C contains a calcium stearate (less 0.5%), sample Z contains a zinc stearate (less 0.5%) which melts at a lower temperature (130°C) than calcium stearate (179°C). We do not know enough about the influence of the melting point, when the additive is distributed on a molecular scale. The samples are highly stabilized. The molecular weight distribution, of course, is the same for the two samples (Fig. 2). The differences between the curves demonstrate the difficulties in measuring molecular weight distributions.

TABLE 1: Branching of LDPE samples (ICI).

Sample	Total CH_3/1000C	Ethyl branches/1000C	Butyl branches/1000C	Amyl branches/1000	>C6 branches per 1000C
IUPAC I	15.2	~1	9.2	2.1	2.9
IUPAC II	15.8	~1	8.8	2.7	3.3

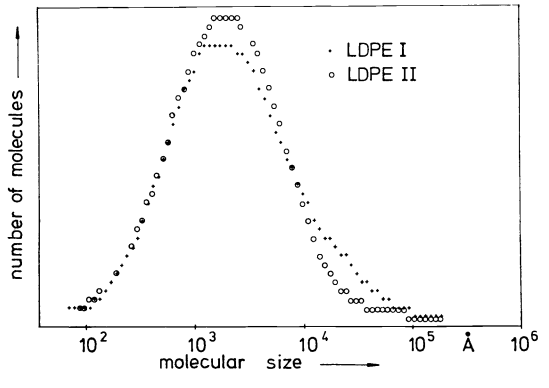

Fig. 1: Molecular size distribution of LDPE (ME)

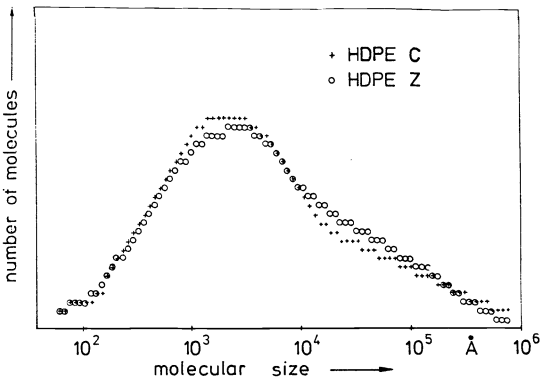

Fig. 2: Molecular size distribution of HDPE (ME).

A careful examination of the GPC measurements shows that the sample C seems to be more soluable than sample Z (concentration 0.25% for C instead of 0.125% for Z at CdF laboratory). The higher concentration might be the reason for differences in the GPC-data between C and Z.

3. FILM BLOWING EXPERIMENTS

The technological behavior of the four samples was studied in film blowing under a variety of processing conditions and with respect to the end use properties. The biaxial extension of the polymer is described by the velocity ratio

$$V = v_f/v_o$$

and the blow up ratio

$$A = d_f/d_o.$$

The symbols are explained in the list of notations. Subscripts f and o relate to the solidified (25°C) film and to the condition at die exit, respectively.

Other important parameters of the film blowing experiments are the temperature at the die exit, the mass flow rate, and the distance of the freeze line from the die exit. Additionally, the deformational history in the die preceding to the actual film blowing is known to be very influential (4, 17-19); this makes it very difficult to compare results of different laboratories, since each of them performed experiments with dies of different geometry.

3.1. MAXIMUM EXTENSIBILITY IN BLOWING

The extensibility experiments showed which of the materials has the potential of being processed into thinner film (irrespectively of film quanlity). For continuity reasons, the film thickness

$$s_f = (h_o/VA)\ (\rho_o/\rho_f)$$

is proportional to the gap width h_o of the die. The film thickness s_{min} at break depends on the ratio V/A, i.e. on the drawdown due to large takeup speed (V large) or due to a large bubble diameter (A large). The time of experiment, i.e. the residence time of a material element in the bubble forming zone, depends on the distance of the freeze line from the die exit and on the velocity distribution in the bubble.

The experimental setup of the different laboratories is compared in Table 2. The processing conditions in the different laboratories were the following:

ETH: At a constant extrusion speed v_o and at constant takeup speed v_f ($V = v_f/v_o$ const. as a second parameter) the blowup ratio was increased until the bubble ruptured. Steady processing conditions were defined by a stable operation of the process for 10 minutes.

Hoechst: The bubble diameter was kept constant (constant A) and the takeup velocity v_f was increased at a given extrusion speed. If the maximum takeup velocity was reached without rupturing the bubble, the film thickness was reduced further by reducing the extrusion speed v_o, i.e. by slowing down the speed of rotation of the extruder screw.

IKT: The experimental conditions were chosen to be similar to these used at ETH. The gap width of the die, however, was taken to be h_o = 1 mm instead of h_o = 0.6 mm. This was done to find out whether the film thickness at rupture depends on a maximal drawdown ratio s_f/h_o or just on a minimum value of s, at which the bubble is stable.

TABLE 2: Comparison of the film blowing equipment in three laboratories.

Laboratory	ETH	Hoechst	IKT
Extruder diameter (mm)	30	60	45
Die diameter (mm)	65	120	40
Gap width of die h_o (mm)	0.6	0.8	1.0
Blowup ratio $A = d_f/d_o$	variable	5.8	variable
Velocity ratio $V = v_f/v_o$	variable	variable	variable

Data on LDPE

Both materials can be extrusion blown into very thin film. For sample II the film thickness s_{min} at break was found to be lower than for sample I. The differences between the two samples appeared most pronounced at low blowup ratios and at high extrusion speed v_o (high mass flow rate). These were the conditions of shortest experimental time. The minimal film thickness as a function of the blowup ratio is shown in Fig. 3. At low blowup ratios, the drawdown velocity ratio V has to be large to get a thin film; correspondingly the residence time of the polymer in the bubble forming zone is comparatively small and the strain rates are high.

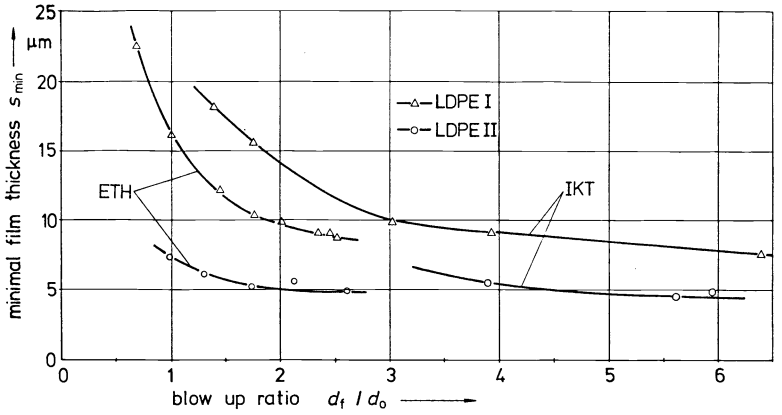

Fig. 3. Minimal film thickness of LDPE samples as a function of blowup ratio; T = 180°C at ETH and T = 190°C at IKT.

Data on HDPE

Both materials can be processed to very thin film. On a large film blowing unit, sample Z is processable to a film of 1.5 µm, while the smallest film thickness of sample C is 4 µm. Continuous operating conditions were achieved at a film thickness of 5 µm for sample Z and at 10-15 µm for sample C (Hoechst). This difference was much less pronounced on a small laboratory film blowing system (ETH), see Fig. 4.

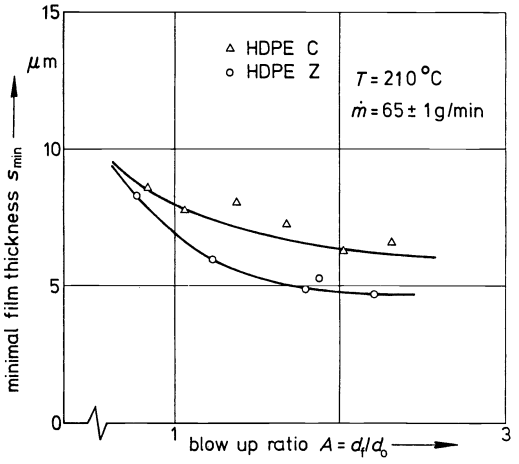

Fig. 4. Minimal film thickness of HDPE samples as a function of blowup ratio (ETH).

3.2. BUBBLE SHAPE, DRAWDOWN FORCE, INTERNAL PRESSURE

3.2.1. FILM BLOWING OF LDPE SAMPLES

The two LDPE samples were blown into film at four different operating conditions (at IKT). The apparatus is specified in Table 2. The testing conditions were

mass flow rate 8.57 kg/h,
melt temperature at die exit 169-175°C,
average velocity at die exit 1.5 m/min.

The operating conditions were reproduced for the two samples: For all experiments the cooling system was operating at flow rates which gave about the same height of the freeze line for comparable runs. The strain in the bubble forming region was modifed by choosing four different combinations of the blow ratio A and the velocity ratio V. The lowest height of the freeze line was achieved with high values VA (see Table 3). The bubble of sample II self-adjusted at much lower freeze lines than sample I. This difference might be due to the different crystallization behavior of the two samples. The temperature distribution is shown in Fig. 5.

The shape of the bubble r(z) was observed, see Fig. 6. It is remarkable that the shapes of the bubbles were quite different for the two samples. This difference in shape, of course, influences the heat transfer between the cooling air stream and the bubble.

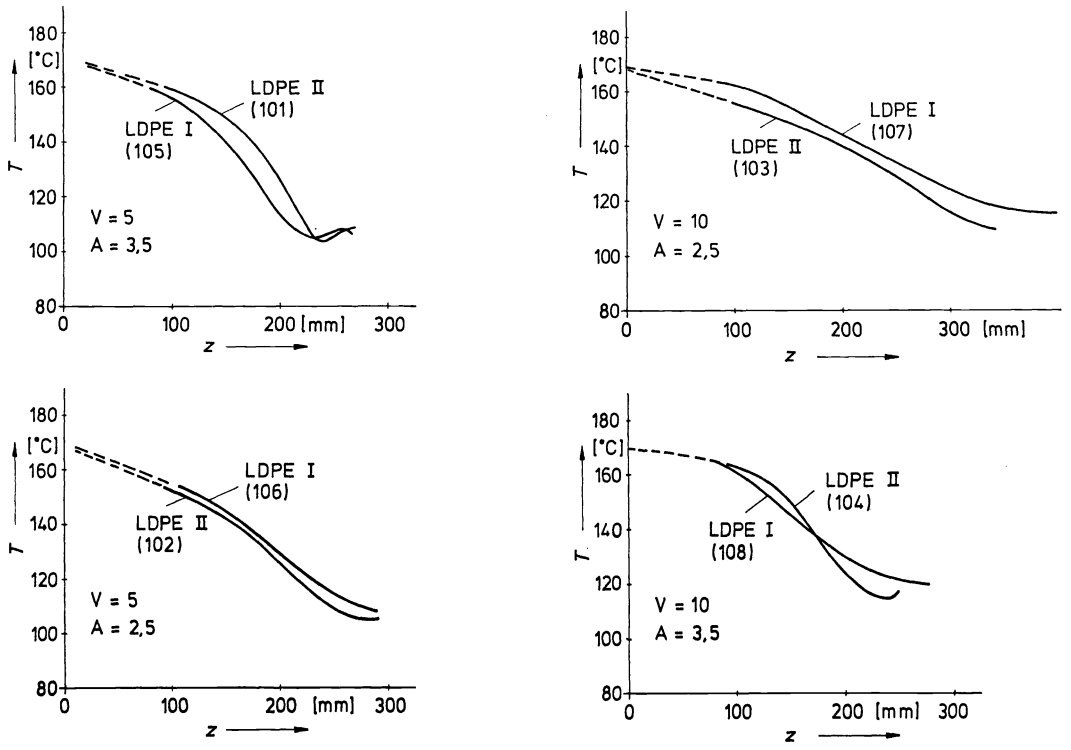

Fig. 5. Film blowing of LDPE samples; temperature distribution along bubble (IKT). For blowing conditions, see table 3.

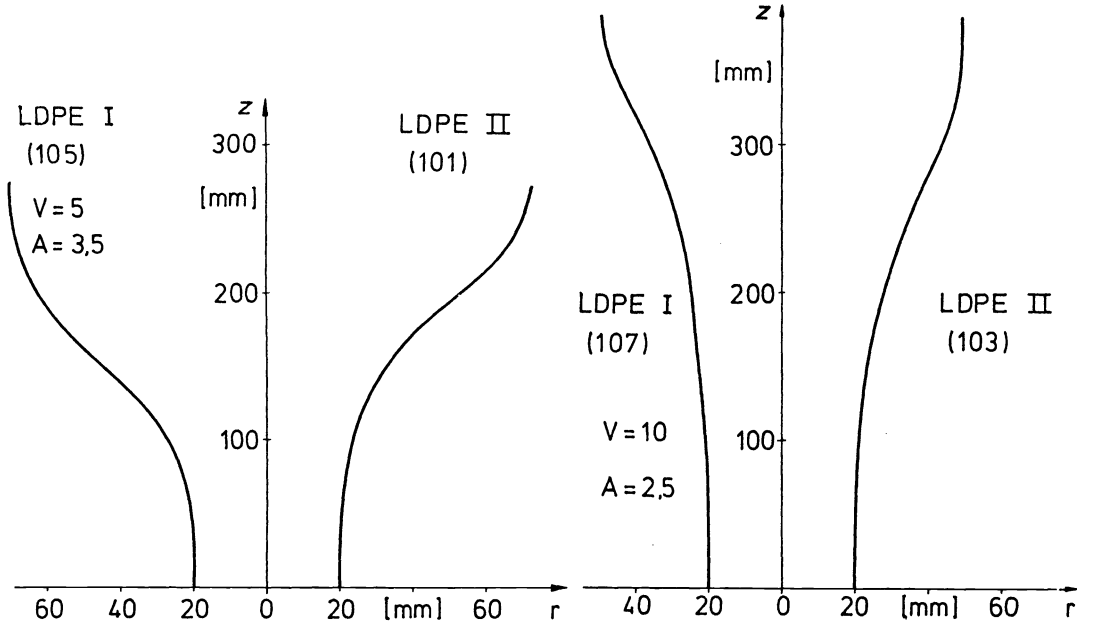

Fig. 6. Bubble shapes r(z) of LDPE samples at two typical blowing conditions (IKT).

TABLE 3. Experimental results of film blowing (IKT).

Material	LDPE I	LDPE II	LDPE I	LDPE II	LDPE I	LDPE II	LDPE I	LDPE II
	A = 2.5 V = 5		A = 2.5 V = 10		A = 3.5 V = 5		A = 3.5 V = 10	
Internal pressure p_i (Pa)	108	110	101	105	106	105	90	100
Freeze line height (cm)	32	27.5	40	33.5	24	25	24	25
Axial force (N)	1.64	1.28	2.02	1.58	1.54	1.07	2.37	1.60
Film thickness (µm)								
measured	60	60	32	25	45	40	20	20
calculated (from ṁ)	73	72	36	35	55	53	28	30

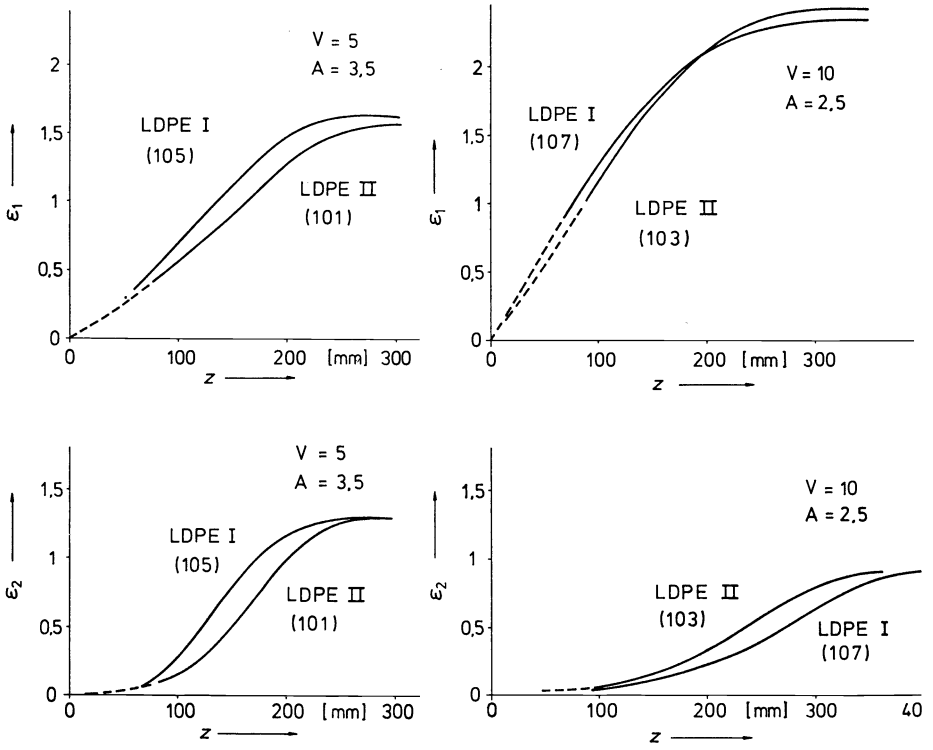

Fig. 7. Film blowing of LDPE (IKT); strain of material element in biaxial extension along the bubble. The strain curves correspond to the bubble shapes shown in fig. 6.

The strain is shown in Fig. 7. The hoop strain $\varepsilon_2 = \ln (r/r_0)$ is calculated from the measured bubble shape and the axial strain $\varepsilon_1 = \ln (v/v_0)$ is calculated from the velocity distribution v(z) along the bubble. The total extension of the material is prescribed by the choice of V and A. In the experiments, they were the same for the two samples. However, the rates of strain and the corresponding temperatures were different. At small blowup ratios, sample I extended more slowly (at high temperature), while at high blowup ratios sample I extended at a higher rate than sample II.

Further results are given in Table 3. The internal pressure was the same or somewhat lower with sample I, while the axial force was significantly higher with sample I.

3.2.2. FILM BLOWING OF HDPE SAMPLES (IKT)

The samples HDPE C and Z were blown to a film of an average thickness 17 µm at a constant mass flow rate, varying blow up ratio A, and varying velocity of the wind up. The testing conditions and experimental results are listed in Table 4. The extrusion die had a diameter of 46 mm and a gap width of 0.6 mm (different than the die for the LDPE film blowing).

TABLE 4. Film blowing conditions for HDPE samples and experimental results (IKT).

Run	701	704	702	705	703	706
Material: HDPE	C	Z	C	Z	C	Z
Blow up ratio A	3		4		5	
Velocity of the film(m/min)	9.5		7.1		5.7	
Freeze line distance (mm)	250		250		200	250
Axial force F_E(N)	3.46	2.46	2.50	1.64	1.88	0.31
Internal pressure p_i (Pa)	220	175	175	150	155	115
Shrinkage in flow direction	0.693	0.696	0.662	0.672	0.650	0.622
Shrinkage in circumferential direction	0.11	0.089	0.114	0.127	0.101	0.113

Temperature distributions along the bubble were measured with an infrared pyrometer, see Fig. 8. The differences in temperature are reflected in the differences in bubble shape.

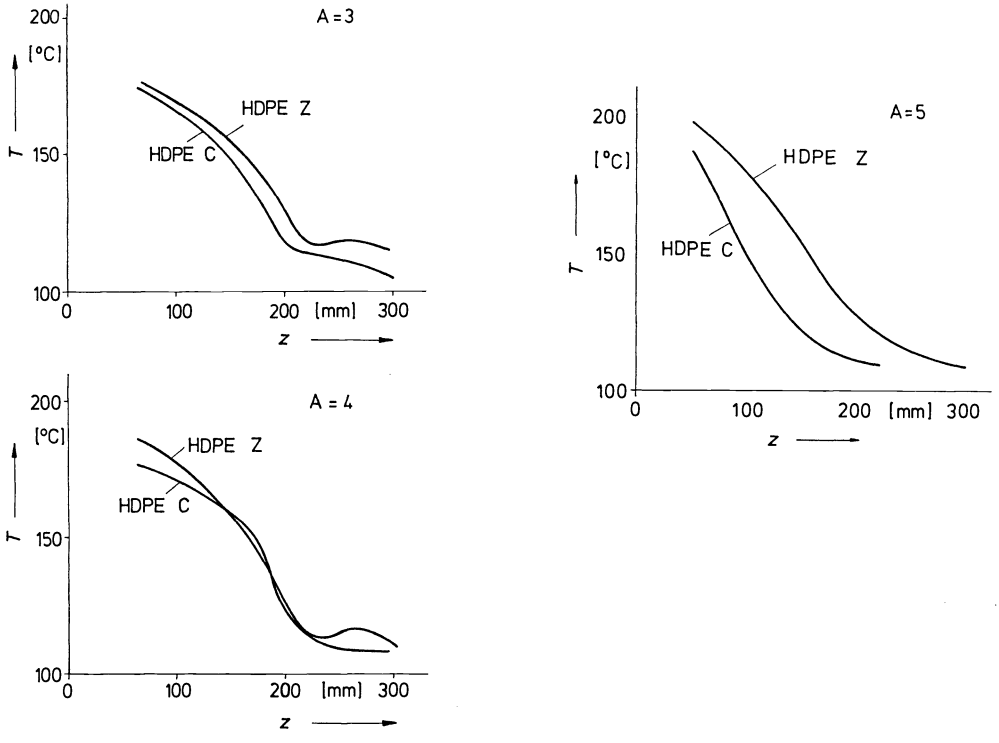

Fig. 8. Temperature distributions in HDPE film blowing (IKT). The blowing conditions are listed in table 4.

The bubble shape as a function of testing conditions (Fig. 9) and the velocity distribution in the bubble (Fig. 10) were measured with a video camera and tracer particles on the film. Each bubble shape and velocity distribution is given by a set of several experiments. The reproducibility of the experiments is very good for the blow up ratios A = 3 and 4, and it is sufficient for the blow up ratio A = 5. The hoop strain ε_2 and the axial strain ε_1 are calculated from the bubble shape and the velocity distribution, respectively. The strains are compared in Fig. 11.

The film thickness distribution in circumferential direction was measured with a mechanical thickness gauge. The variations in thickness are found to be large (about $\pm$ 25%); they increase with increasing blow up ratio, (ICHP).

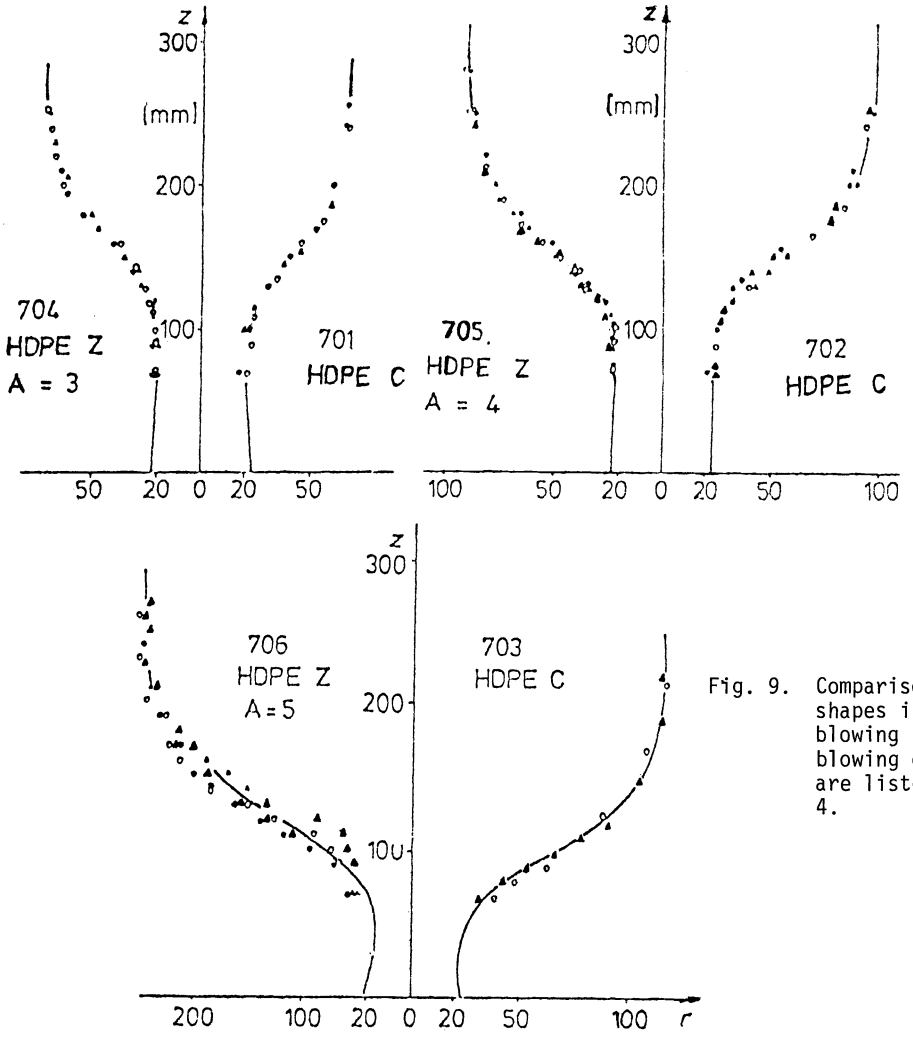

Fig. 9. Comparison of bubble shapes in HDPE film blowing (IKT). The blowing conditions are listed in Table 4.

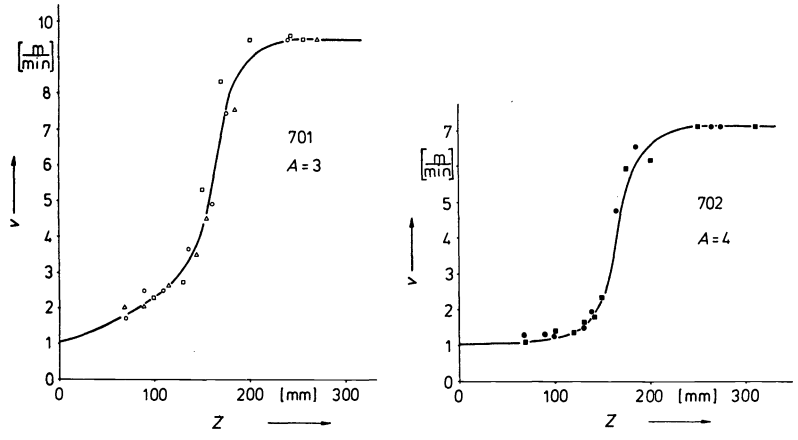

Fig. 10. Axial velocity as a function of the distance from the die exit, z, (IKT). The blowing conditions of the HDPE samples are listed in table 4. Figure is continued on next page.

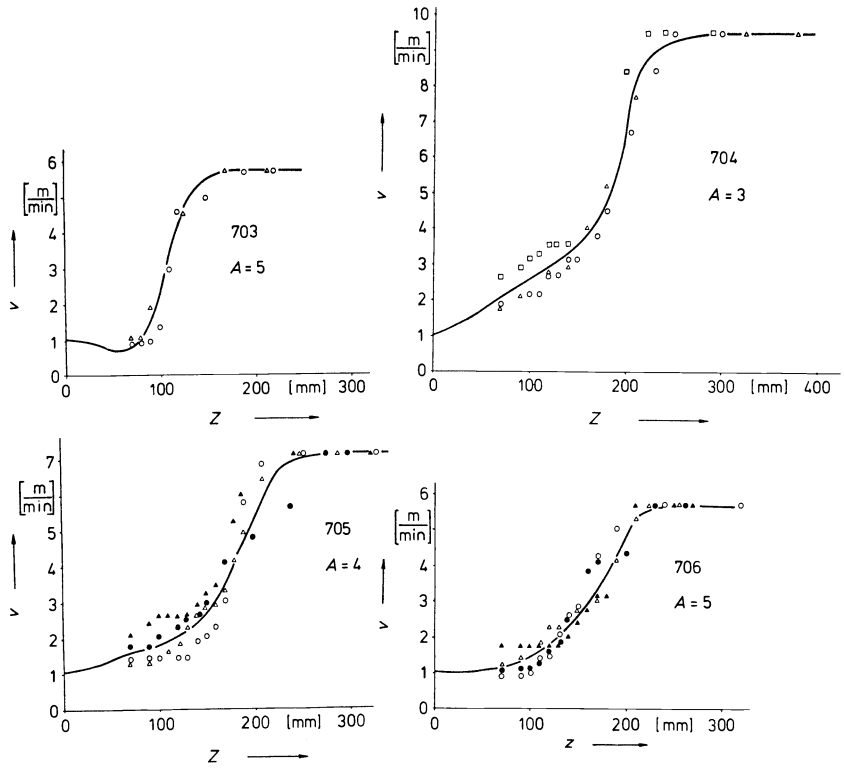

Fig. 10. Continued from previous page.

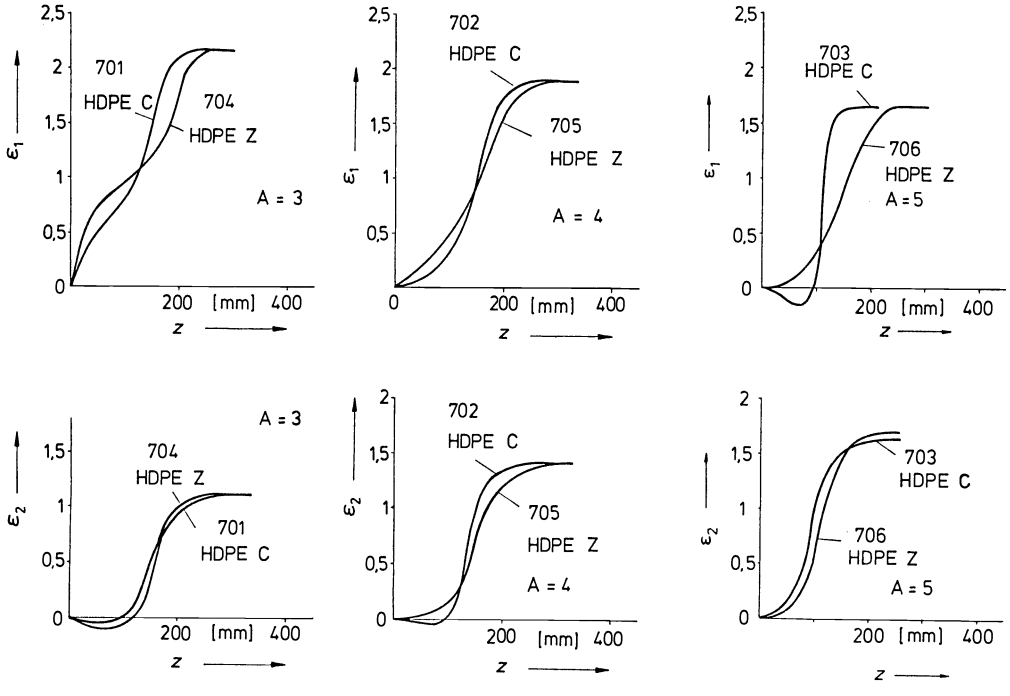

Fig. 11. Hoop strain $\varepsilon_2 = \ln (r/r_0)$ and axial strain $\varepsilon_1 = \ln (v/v_0)$ as a function of distance from the die exit, calculated from data of fig. 9 and fig. 10.

3.3. END USE PROPERTIES

ICI remelted samples of the LDPE film (made at IKT) at 180°C to allow frozen-in orientation to retract. The retraction ratios in both machine and transverse directions were measured to give an estimate of the orientation in the film. The results indicate slightly lower orientations in Sample II,see Table 5. All samples were found to be substantially oriented in machine direction.

TABLE 5: Retraction ratio of LDPE film samples (ICI); MD = machine direction, TD = transverse direction.

Run	LDPE sample	A	V	Retraction ratio MD	TD
106	I	2.5	5	4.2	1.4
107	I	2.5	10	5.6	1.5
105	I	3.5	5	4.5	1.5
108	I	3.5	10	7.1	1.6
102	II	2.5	5	4.0	1.2
103	II	2.5	10	5.6	1.5
101	II	3.5	5	3.7	1.6
104	II	3.5	10	5.0	1.9

The tensile impact strength of the HDPE films (s = 20 μm) was measured; the results are shown in Table 6. There seem to be large differences between C and Z, since variation of stem length does not affect the impact strength of sample C, but for sample Z the stem length was found to have a large effect in the transverse direction. The addition of zinc stearate instead of calcium stearate produces a much "tougher" film. The visual examination of the optical properties of the films yields that the films of sample C have structures and matter surfaces than those of sample Z.

TABLE 6: Tensile impact strength of HDPE samples at two bubble stem lengths (Hoechst).

Sample	Stem length (cm)	Tensile impact strength (kJm^{-2}) longitudinal	transverse
C	20	3400	430
	50	2900	410
Z	20	2900	600
	50	3600	3100

Shrinkage tests on the films blown at IKT do not show significant differences between samples C and Z. The shrinkage values in Table 4 are defined as relative change in length $\Delta\ell/\ell_0$ of the samples in shrinkage tests.

3.4. CONCLUSIONS FOR THE FILM BLOWING EXPERIMENTS

The film blowing experiment consists of two parts: (1) the blowing of the thinnest film possible at steady operating conditions,and (2) the blowing of films at various operating conditions and the measurement of end use properties.

Each of the samples could be blown into thin film. The thinnest film was achieved at low take up speed and high blow up ratio. Both pairs of samples showed significant differences in this test. Sample II gave the thinnest LDPE film and sample Z the thinnest HDPE film. Differences in film blowing performance were much more pronounced on a large film blowing unit than on a small laboratory system.

Four operating points (blow up ratio A, velocity ratio V) were chosen for blowing LDPE films. The bubble shapes and the temperature distribution in the bubble are most sensitive to the molecular differences between the two samples. LDPE I behaved more stable in the film blowing. The shrinkage properties are about the same for the two films.

Three operating points (A, V) were chosen for testing the film blowing behavior of the HDPE samples. The bubble shape and the temperature distribution along the bubble were found to be different between the two samples. These differences, however, were not reflected in the shrinkage properties of the films.

Mechanical testing showed that the impact strength of film Z was significantly higher than the one of film C. The impact strength was higher for films blown with a long stem of the bubble (only for sample Z).

4. MATERIAL CHARACTERISTICS,CRYSTALLIZATION, AND RHEOLOGICAL EXPERIMENTS

Rheological experiments require a stability test, which makes sure that the rheological properties do not change during a rheological test. The duration of most rheological tests is much longer than the average residence time in processing equipment.

Crystallization has been studied under isothermal and transient temperature conditions.

The rheological experiments are divided into two groups: shear and elongation. Shear flow experiments with capillaries give additional data like pressure drop in converging flow and extrudate swell.

4.1.THERMAL STABILITY TEST

ETH tested the thermal stability of the LDPE samples at 190°C by measuring the MFI (190°C/2.16 kg) at different residence times. The first measurement was made after 4 minutes according to ISO 1133. Thermal stability at 190°C seemed to be sufficient for both LDPE samples up to 200 minutes; for larger residence times the melt index decreased rapidly (Fig. 12). Oscillatory measurement (G', G" at $\omega = 7.9 \times 10^{-3}\ s^{-1}$) confirm the thermal stability of the LDPE samples at 150°C up to 200 minutes (Shell). G' is the more sensitive material function when monitoring material changes with time.

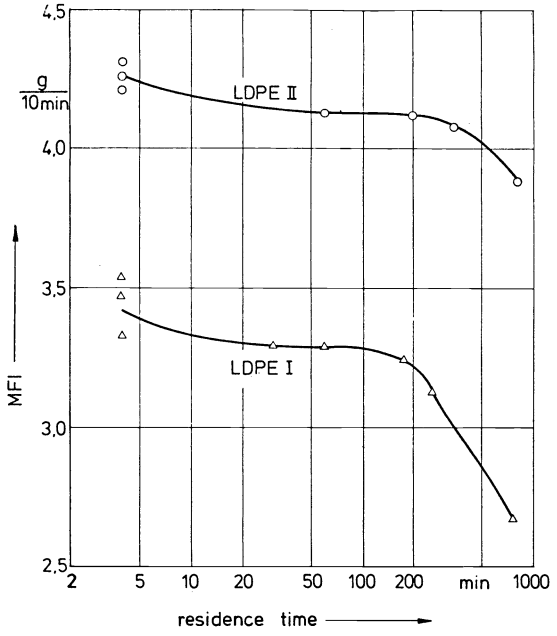

Fig. 12. Stability test; melt flow index MFI 190°C/2.16 kg as a function of residence time of the polymer in the apparatus (ETH).

Thermal stability was monitored by measuring the mass flow rate as a function of the residence time in the barrel of a nitrogen gas-driven capillary viscometer (BASF). The measurements began after a preheating time of about 10 minutes. The LDPE samples possess a satisfying thermal stability at 240°C up to a residence time of at least 90 minutes (Fig. 13). The HDPE samples are sufficiently stable at temperatures of 180°C up to 90 minutes. The mass flow rate of HDPE C is higher than that of HDPE Z at T = 180°C, but lower at T = 220°C (Fig. 14). These differences could not be found on a piston-driven rheometer (Hoechst).

4.2. CRYSTALLIZATION TEMPERATURE, CRYSTALLIZATION BEHAVIOR IN SHEAR AND EXTENSIONAL FLOW, DSC MEASUREMENTS

The crystallization temperature is a significant parameter of the film blowing process; it terminates the deformation of the film at the freeze line. The crystallization process influences the bubble shape. However, it remains open as to how the crystallization behavior relates to the maximum drawdown, since the rupture occurs close to the exit of the film blowing die.

For measuring the crystallization temperature (at CWH), the samples were molded between two glass plates of distance 50-60 µm. The upper plate could be moved with a frequency of 0.25 Hz and an amplitude of 225 µm. In a dynamic crystallization experiment, the samples were cooled down with constant cooling rates of 0.7, 2.5, 7.2, and 22 K/min. From the variation of the intensity of a light beam transmitted by the sample, the temperatures of beginning of crystallization T_1 and end of crystallization T_2 were measured. A typical light intensity curve is shown in Fig. 15.

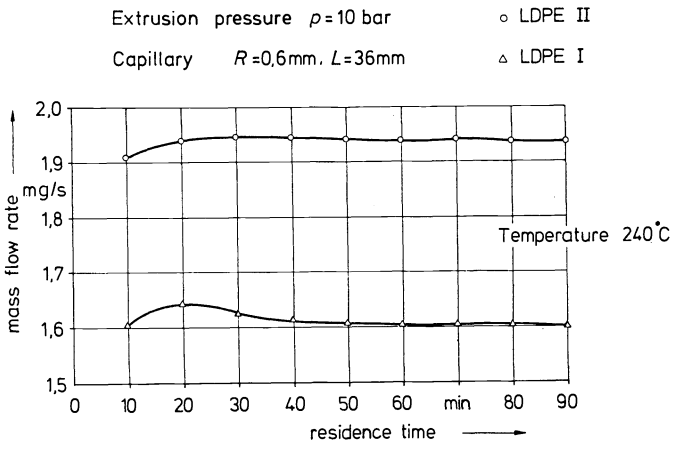

Fig. 13. Stability test; mass flow rate through capillary at constant extrusion pressure and varying residence times for LDPE I and II (BASF).

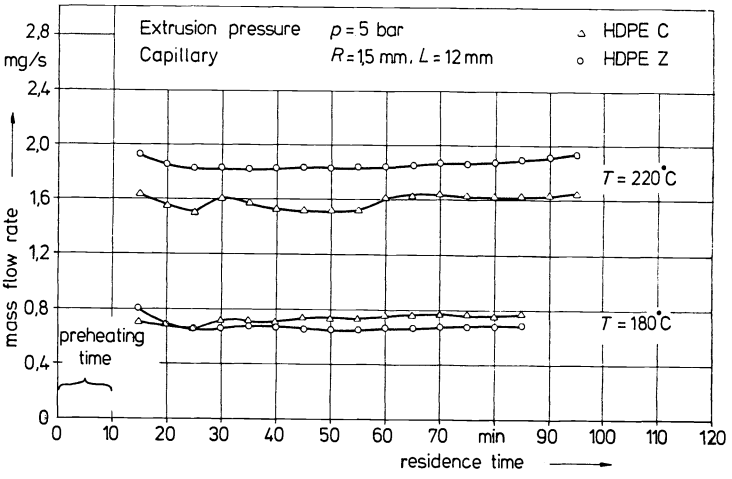

Fig. 14. Stability test; mass flow rate through capillary at constant extrusion pressure and varying residence times for HDPE C and Z (BASF).

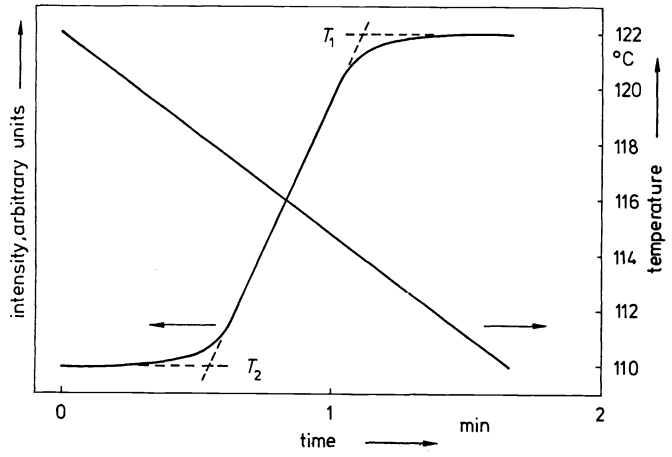

Fig. 15. Typical intensity curve for dynamic crystallization experiment (CWH).

In Fig. 16 and Fig. 17, the temperatures T_1 and T_2 are displayed as a function of the cooling rate. The accuracy of the data is within ± 0.8 K. The crystallization temperatures are significantly lowered at high cooling rates (see also Table 8). An inspection of the figures shows that the two LDPE samples do not exhibit significant differences, except at very low cooling rates. This result is confirmed by Magill and Peddada (3) on the PE samples of the preceding film blowing study (1). Oscillatory shear does not influence the crystallization process. However, there appeared significant differences between the HDPE samples, especially at high cooling rates. Oscillatory shear slightly increases the crystallization temperature (see Table 7).

TABLE 7. Temperatures T_1 and T_2 of beginning of crystallization and of end of crystallization at different cooling rates, with and without shear. Spherulitic radii (CWH).

Sample	Cooling Rate K/min	without shear		under shear		spherulitic radium $\bar{R}$ µm	
		T_1 °C	T_2 °C	T_1 °C	T_2 °C	without shear	under shear
C	0.7	121	117	127	122	7.9	
	2.5	119	117	124	115	6.8	
	7.2	120	115	120	116	5.9	5.9
	22.0	119	115	120	116	4.5	4.7
Z	0.7	122	119	128	120	9.5	
	2.5	121	116	125	118	9.5	5.9
	7.2	118	114	119	116	7.6	
	22.0	115	112	115	112	6.3	4.5
I	0.7	105	100	108	103	13.6	
	2.5	104	98	105	102	13.6	
	7.2	102	99	104	99	11.8	4.7
	22.0	101	97	101	97	9.5	9.5
II	0.7	107	103	109	104	13.6	13.5
	2.5	105	102	107	103	15.8	10
	7.2	103	99	104	101	15.8	6.8
	22.0	99	97	100	97	9.5	10

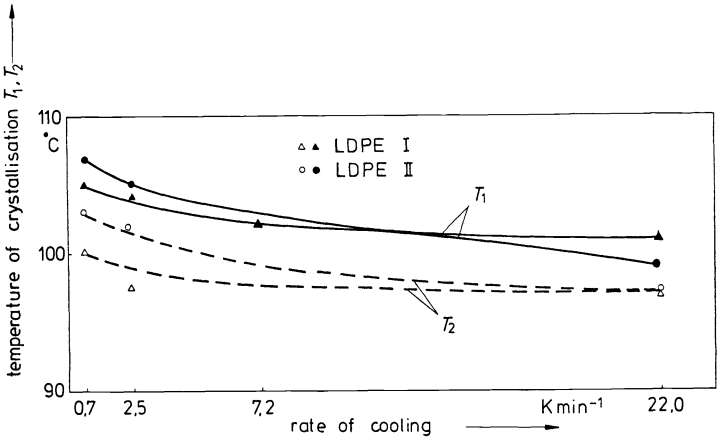

Fig. 16. Temperature T_1 of beginning of crystallization and temperature T_2 of end of crystallization at different rate of cooling (CWH). Date for shear and without shear are indistinguishable.

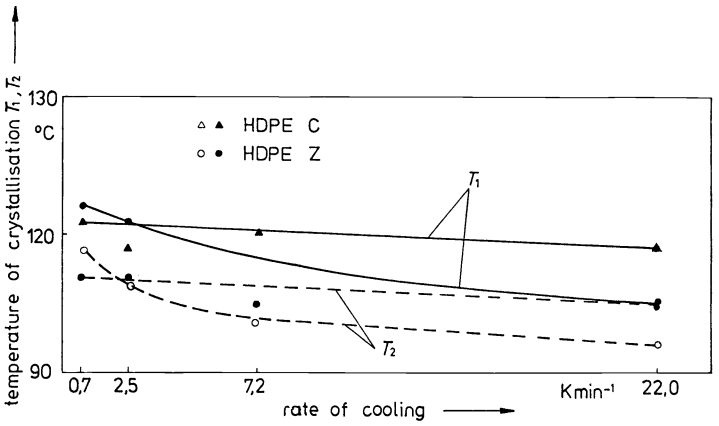

Fig. 17. Temperature T_1 of beginning of crystallization and temperature T_2 of end of crystallization at different rate of cooling (CWH). Data with shear.

The spherulitic radii as a function of cooling rate are displayed in Fig. 18. Comparing the samples, the values of HDPE Z are higher than those of HDPE C but converging towards higher cooling rates, while the values of LDPE II are higher than those of LDPE I throughout. Spherulitic radii have been determined by CWH from the small angle light scattering. The values are listed in Table 6 together with the results of T_1 and T_2 with and without shear.

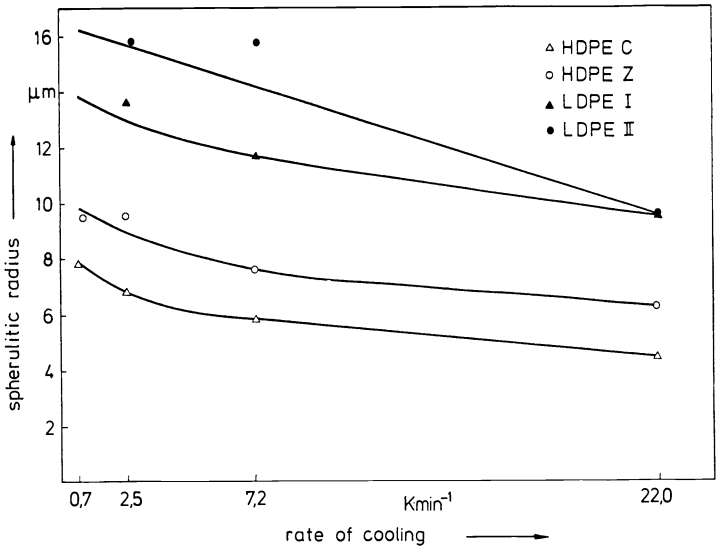

Fig. 18. Spherulitic radii as a function of cooling rate (CWH).

A second laboratory (ME) performed dynamic crystallization experiments on the HDPE samples using the Perkin-Elmer DSC 1B calorimeter. The polymer was conditioned for 5 min at 150°C and then cooled down at the controlled speeds of 8 and 64 K/min. The temperatures of beginning of crystallization T_1 and the crystallization peak T_{max} were determined. These temperatures seemed to be practically the same for samples C and Z (see Table 8).

A third laboratory (BASF) performed dynamic crystallization experiments using a DSC 1B calorimeter. The operating conditions were the same as in the laboratorium of ME. The sample weight was 2 mg, and the results were corrected for inertia of the instrument (20). The temperatures T_1 and T_{max} of initiation of crystallization and of the crystallization maximum, respectively, are shown in Fig. 19. The rate of crystallization of C is smaller at slow cooling and larger at high cooling rates. The trend of these results is the same as in the experiments by ME, but the observed differences between the two HDPE samples were much smaller than in the experiments of ME.

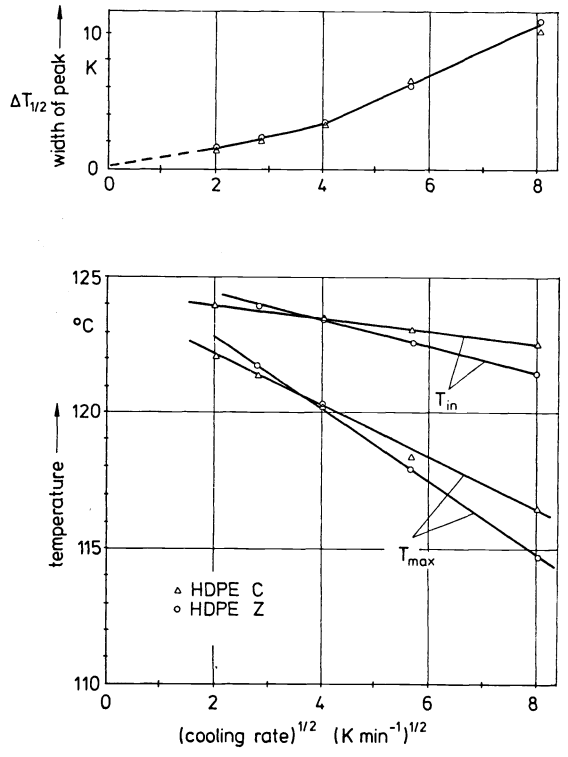

Fig. 19. Dynamic crystallization of HDPE C and Z (BASF): Temperature of initiation of crystallization and temperature of maximum crystallization rate as a function of cooling rate. $\Delta T_{1/2}$ is the width of the crystallization peak.

TABLE 8. Dynamic calorimetry with Perkin Elmer DSC 1 B. Temperature T_1 of beginning of crystallization and temperature T_{max} of crystallization peak (ME, BASF).

Sample	Cooling rate (K/min)	T_1 (°C) ME	BASF	T_{max} (°C) ME	BASF
HDPE C	8	118	124.0	114	121.4
C	64	104	122.5	92	116.5
HDPE Z	8	119	124.0	114	121.8
Z	64	103	121.5	92	114.6

Isothermal crystallization was studied by four laboratories (BAS, Hoechst, ICI, ME). At ME the HDPE samples were conditioned at 150°C for 5 min and the crystallization process in isothermal conditions was recorded at 120, 121, and 122°C (uncorrected dial reading). Both polymers showed, as reported by ICI in the next section, a double crystallization process which is more evident for sample Z than for sample C; the times at which two peaks occurred are reported in Table 9; however, the data have only indicative values since the temperature values of the DSC 1B could not be fixed with a great degree of accuracy.

TABLE 9. Isothermal calorimetry with Perkin Elmer DSC 1 B by ME.

Material	HDPE C		HDPE Z	
Temperature	peak 1	peak 2	peak 1	peak 2
122°C	2'10"	19'40"	1'40"	12'10"
121°C	40"	6'30"	40"	6'50"
120°C	30"	2'30"	20"	2'40"

The birefringence was measured by ICI during an isothermal crystallization at 121°C, using an optical hot stage equipped with a photo multiplier. The crystallization occurred in two stages: Almost immediately a small degree of birefringence was observed, this increased towards a maximum over a time scale 't' at which a much more rapid increase in briefringence was observed. The time scale 't' for sample C was significantly shorter than for sample Z:30.5±0.5 s versus 40.0±2.0 s.

In a third laboratory (Hoechst) the HDPE samples were conditioned for 5 min at 190°C and then cooled down with controlled speed of 64 K/min to the crystallization temperature. Counting of time was started when the chosen temperature was reached (indicated by ceasing of base line drift). The heat flux was integrated to different elapsed times to give the crystallization enthalpy H, and $\Delta H_t/\Delta H_\infty$ was plotted against time t. The half time of crystallization is defined as the time for which $H_t = 0.5\ \Delta H_\infty$. The results indicate that the sample with the higher crystallization rate reached a higher degree of crystallinity. The rate of crystallization was characterized by the half-time of the transition, which is plotted as a function of temperature in Fig. 20. Sample Z crystallized at a higher rate than sample C; there was no sign that crystallization occurred in two steps contrary to the isothermal crystallization experiments as described above. The crystallization enthalpy was evaluated over the temperature range and is given in Fig. 21.

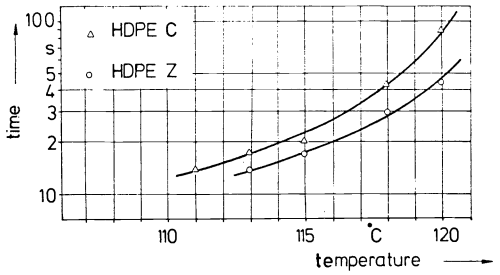

Fig. 20. Crystallization behavior of HDPE samples: Half time of crystallization (Hoechst).

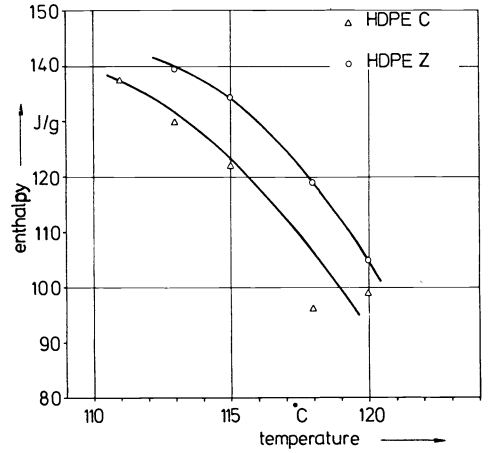

Fig. 21. Crystallization enthalpy as a function of temperature (Hoechst).

BASF studied isothermal crystallization of HDPE C and Z at 120.7 ± 0.2°C. The experimental conditions were similar to these at Hoechst. The half times of crystallization were found to be about the same for C and Z (43s versus 40s). This result is in contradiction to the findings at Hoechst which reported half times of 100s for C and 50s for Z. BASF did not observe two stages in the crystallization process.

The flow-induced crystallization behavior of the samples was shown by Shell using an Instron capillary rheometer (21). The capillaries have diameters of 1.27 mm for the LDPE samples and 3.0 mm for the HDPE samples (L/D = 40 and entry angle of 90° in both cases). The samples were first heated to a temperature of 190°C, which is well above the melting points of the polyethylene samples, and kept at that temperature for 5 min. Subsequently the samples were cooled down to the test temperature (110°C for LDPE and 140°C for HDPE) which took about 10 min. The plunger speed (flow rate) was then continuously increased until crystallization of the samples stopped further flow.

Fig. 22 shows the results of the flow-induced crystallization experiments at 110°C. It demonstrates that LDPE II has the lowest viscosity, and starts to crystallize at a lower shear stress than sample I. A steep rise in viscosity towards infinity at a given shear rate (flow rate) is denoted in this plot by a line having a positive slope of 45°, since both viscosity and shear stress increase by the same amount. The differences in the onset of flow-induced crystallization are quite small but nevertheless reflect some differences in molecular structure between the two LDPE samples.

Fig. 23 shows the results of the flow-induced crystallization experiments at 140°C. It can be seen that at 140°C the viscosities of both HDPE samples are about equal. Moreover, it follows from Fig. 23 that HDPE Z is more sensitive to flow induced crystallization than sample C. At an apparent shear rate of 4.5 s^{-1}, for instance, sample C crystallized very slowly while the crystallization of sample Z was so fast that it readily stopped further flow. Another difference between sample C and sample Z was that in the case of sample C the flow curve returned to normal behavior at higher shear rates which might be due to slip at the wall or viscous dissipation in the capillary causing melting of the initially formed crystallites.

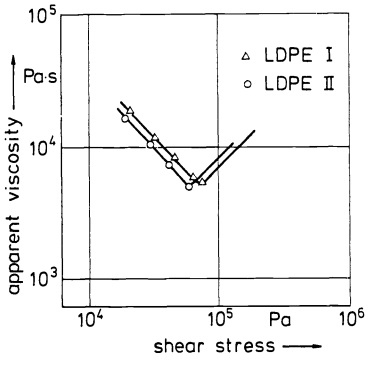

Fig. 22. Apparent viscosity as function of wall shear stress at 110°C. In the experiment, the flow rate is increased until crystallization stops further flow (Shell).

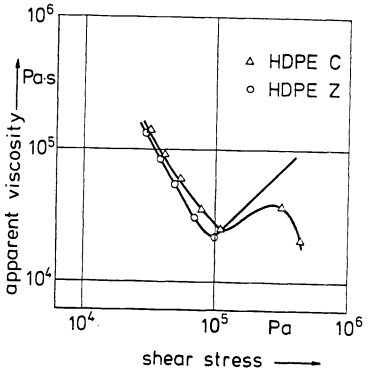

Fig. 23. Apparent viscosity as function of wall shear stress at 140°C. In the experiment, the flow rate is increased until crystallization stops further flow (Shell).

One laboratory (ICI) found that HDPE C seems to be slightly whiter than sample Z and made a quantitative comparison to test this structural difference between the HDPE samples by using a color difference meter which showed reflectances in the ranges of Table 10. Ten probes were evaluated in each case, so that the results appear to be significant. It is anticipated that the difference in whiteness might be associated with sample C containing many more nuclei than sample Z.

TABLE 10: Reflectance of HDPE samples (ICI). The numbers are given in % of the intensity of the incoming light of the color green, red or blue.

Sample	Intensity of Reflected Light		
	Green	Red	Blue
HDPE C	60.5 - 60.9	60.9 - 61.3	56.3 - 56.6
HDPE Z	57.9 - 58.9	57.9 - 59.3	53.4 - 54.8

Conclusions of crystallization experiments

A variety of tests are used to study the crystallization behavior. Differences in experimental procedure make it difficult to reach a satisfying agreement between participating laboratories.

The LDPE samples seem to be very similar in their crystallization behavior. Sample I crystallizes at slightly lower temperatures (dynamic crystallization at low cooling rates) and at slightly higher shear stress (shear induced crystallization in capillary flow). The spherulitic radii of sample I are lower, at least when cooling slowly from the melt.

The HDPE samples showed contradictory crystallization behavior. Samples C seems to exhibit lower (CWH) or the same (ME,BASF) crystallization temperatures. A double crystallization

process has been observed by ICI and ME, while BASF and Hoechst did not find this behavior. This difference might be due to sample preparation: At BASF and Hoechst the samples were preheated up to 190°C, while ICI and ME heated the samples to 150°C only. Annealing at 190°C might have erased the memory on sample preparation while at 150°C the memory is maintained. Sample C requires higher shear stresses for shear induced crystallization in capillary flow.

4.3.. PROPERTIES IN SHEAR AND IN RELATED TESTS

The samples were tested in simple shear, unsteady and steady as well. The shear related tests are determined by shear flow with some extensional flow superimposed. For these mixed flows, the shear may occur in the experiment itself (melt index, entrance pressure loss on capillaries) or in the preceding flow history (extrudate swell).

4.3.1. MELT FLOW INDEX (2.16 kg/190°C)

The melt flow index is listed in Table 11. LDPE I has a lower melt index than LDPE II. The differences are quite larger, even at high temperatures. This already indicates differences within this LDPE-pair which are larger than within the LDPE samples A,B,C of the preceding study (1). HDPE C has about the same melt index as sample Z.

TABLE 11: Melt index as measured in different laboratories

Temperature	LDPE I	LDPE II	HDPE C	HDPE Z	Laboratory	Time (min)	Weight (kg)	Die
190°C	3.41	4.22	0.066	0.059	ME	10	2.16	STD
130°C	7.5	9.8	-	-	ICI	6	10	STD
210°C	-	-	2.0±0.3	2.1±0.3	ETH	10	2.16 for LDPE; 10 for HDPE	
190°C	3.47±0.1	4.3±0.1	1.2±0.2	1.3±0.2				
180°C	2.51	2.99	1.05	1.12				
150°C	1.07	1.27	0.51	0.6				
120°C	0.31	0.35	-	-				
190°C	-	-	0.26	0.28	Hoechst	-	5	-

4.3.2. VISCOSITY IN STEADY SHEAR, FLOW CURVE

The viscosity η was measured with the Weissenberg Rheogoniometer (WRG) at shear rates up to $\dot{\gamma} = 0.586\ s^{-1}$ and with various types of capillary viscometers at shear rates above $0.5\ s^{-1}$. The pressure gradient in capillaries (circular and slit cross section) was determined by means of a Bagley plot or by a direct measurement of the axial pressure distribution along the capillary. The shear rates are corrected with the Rabinowitsch method (LDPE) or just taken to be the reduced volume flow rates (HDPE).

Data on LDPE

The viscosity curves measured in different laboratories are plotted in Fig. 24. For shear rates above $10\ s^{-1}$, the viscosity curves are practically the same for the two samples. At low shear rates, the viscosity curves differ significantly; at T = 150°C and $\dot{\gamma} = 5 \times 10^{-3}\ s^{-1}$ the difference is about 30%. Note that lowering the temperature from 150°C to 120°C does not give a significant viscosity increase. However, between 120°C and 115°C the viscosity increases significantly. The viscosity of LDPE II is then significantly higher than the viscosity of LDPE I. This could be due to flow induced in crystallization.

Data on HDPE

In the flow curve, the apparent shear rate at the wall (reduced flow rate $4\ \dot{V}/\pi R^3$) is plotted over the shear stress at the wall. The flow curves as shown in Fig. 25 are practically the same for the two samples. Above a certain shear stress, there appears some instability which might be due to an irregularity in the polymer layer near the wall (22). Below that stress the velocity profile in the capiliary is unperturbed, and a viscosity curve can be determined. A small effect of temperature can be seen: at higher temperature (180°C), the flow curve is slightly higher and it is stable to higher shear stresses.

ETH measured relatively high pressure drops, when the capillary was clean. After several runs, the pressure readings adjusted on reproducible lower levels. It is anticipated that some additive is forming a layer on the capillary surface. The same phenomenon has been observed by Hoechst.

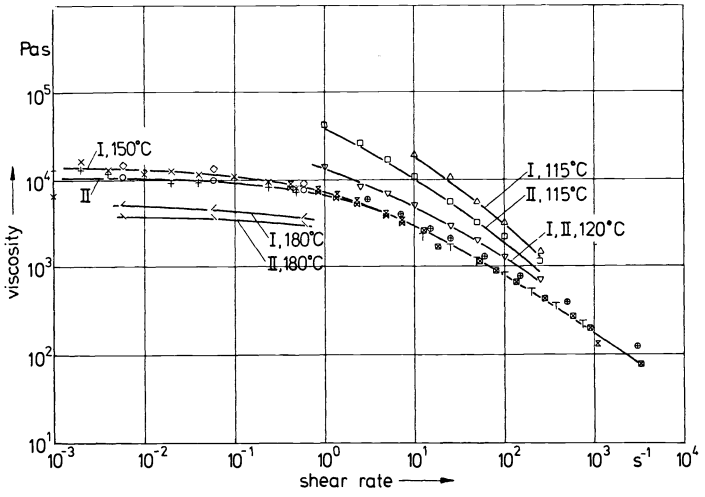

Fig. 24. Shear viscosity of LDPE samples as function of shear rate (TNO, ICI, BASF).

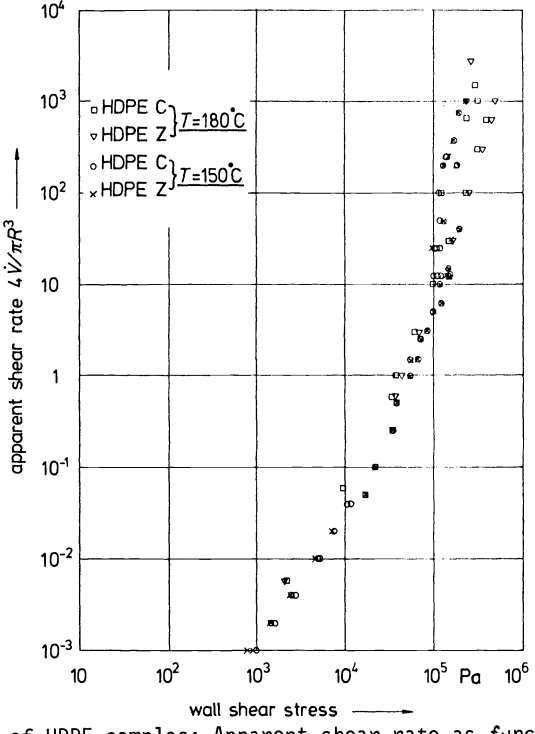

Fig. 25. Flow curves of HDPE samples: Apparent shear rate as function of wall shear stress in capillary flow (TNO, ME, ICI, BASF).

4.3.3. FIRST NORMAL STRESS DIFFERENCE IN SHEAR

The first normal stress difference was measured in a cone and plate rheometer. The results are given in Fig. 26. At a shear rate of 1 s^{-1}, the differences between the two LDPE samples are within the range of accuracy of the experiment. At lower shear rates, however, the normal stress difference becomes almost twice for LDPE I (at $\dot{\gamma}$ = 0.1 s^{-1}).

4.3.4. DYNAMIC EXPERIMENTS (G' AND G")

Dynamic measurements of the storage modulus G' and the loss modulus G" in shear were performed with a cone and plate rotational rheometer and with an eccentric disc apparatus.

Data on LDPE

The storage and the loss moduli of sample I are higher than those of sample II, see Fig. 27 and 28. This difference becomes particularly obvious at small frequencies.

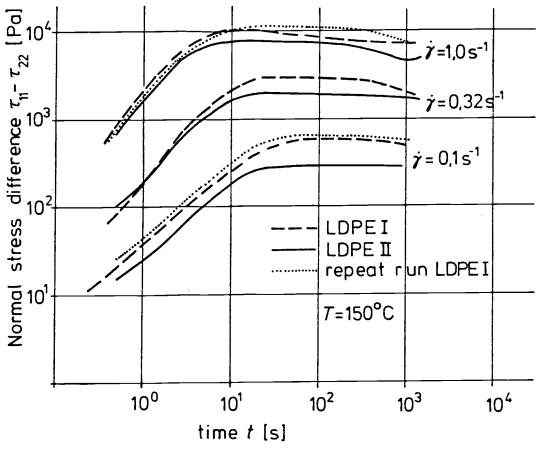

Fig. 26. First normal stress difference of LDPE samples (BASF), T = 150°C. Parameter is shear rate $\dot{\gamma}$. A second run with sample I demonstrates the reproducibility of the experiment.

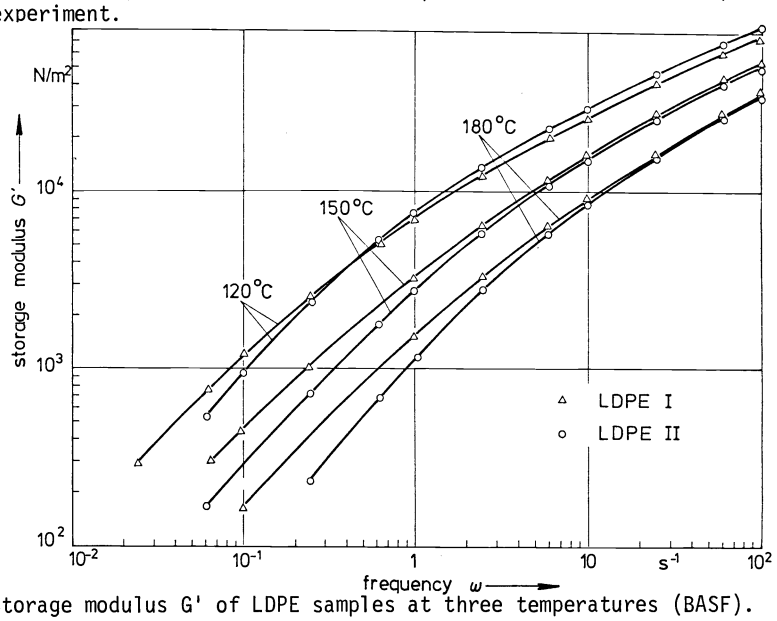

Fig. 27. Storage modulus G' of LDPE samples at three temperatures (BASF).

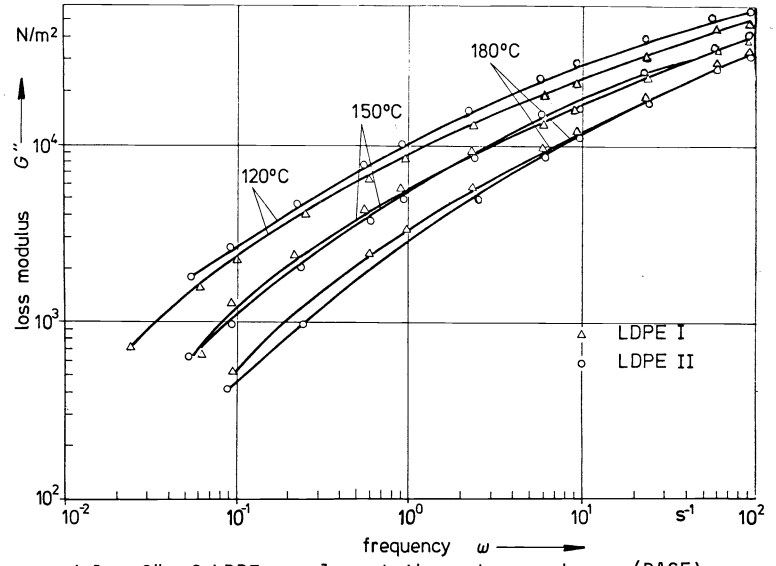

Fig. 28. Loss modulus G" of LDPE samples at three temperatures (BASF).

4.3.5. STRESS GROWTH AT CONSTANT SHEAR RATE, STRESS RELAXATION, AND SHEAR RECOVERY

Stress growth and relaxation experiments at ME were performed by using a WRG R18. The cone angle was $3^{o}56'50"$ and the diameter 50 mm. The stiffness of the torsion bar was 9.43 10^{-5} N m/μm in the case of LDPE samples and 1.06 10^{-3} N m/μm in the case of HDPE samples. LDPE samples have been tested at $150^{o}C$ and $180^{o}C$. HDPE samples have been tested only at $180^{o}C$ because at $150^{o}C$ some slippage of the specimens between cone and plate surfaces occurred. The shear stress and stress relaxation after steady-state flow was measured at three selected values of shear rate: 5.86 10^{-3}, 5.86 10^{-2}, and 5.86 10^{-1} s^{-1}. The stress relaxation experiments began in each case at a total shear strain $\gamma = 8$.

The buildup of shear stress is shown in Figs. 29 and 30. The relaxation behavior is summarized in Fig. 31, where a mean relaxation time (i.e., the time at which the relaxation function $\tau(t)/\tau(0) = 1/e$) is plotted against the shear rate.

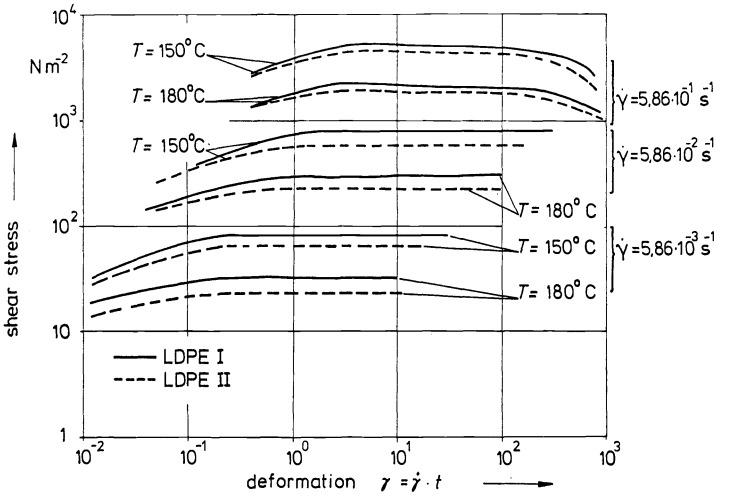

Fig. 29. Stress growth of LDPE samples at three prescribed shear rates, T = $150^{o}C$ and T = $180^{o}C$ (ME).

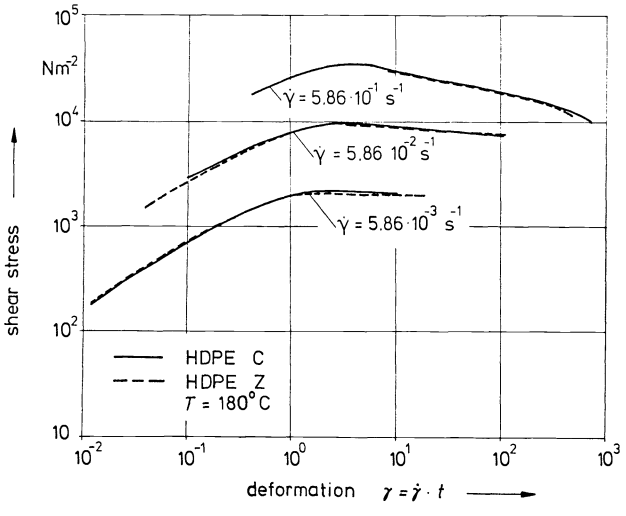

Fig. 30. Stress growth of HDPE samples at three prescribed shear rates (ME).

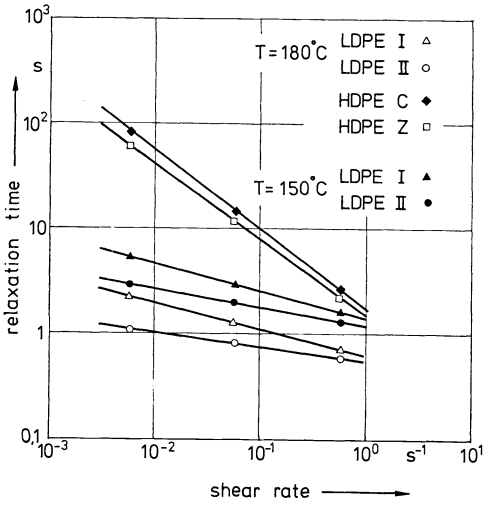

Fig. 31. Relaxation time in stress relaxation after cessation of steady shear. The relaxation time is defined as the time where the shear stress relaxes to 1/e of its steady shear flow value (ME).

Data on LDPE

During stress growth, the shear stress is higher for sample I than for sample II. Correspondingly, the stress relaxes faster in sample II after cessation of steady shear flow.

Data on HDPE

Stress growth and relaxation are about the same for the two samples (ME). Hoechst measured the relaxation modulus in a step shear strain experiment as described by Laun (23). A parallel plate shearing device (simple shear sandwich, total area = 60 cm^2) was used in combination with a tensile testing machine. The relaxation of the stress was measured after steps in shear strain attained at constant shear rate ($\dot{\gamma}$ = 8.33 s^{-1}). There was no difference detected in the relaxation moduli of HDPE C and Z, see Fig. 32.

ICI carried out experiments of constrained recovery after constant shear stress experiments in a cone and plate rheometer. The stress was applied for a time scale which allowed a total deformation of 100 units of shear. Then the stress was removed. Strain recovery was monitored as a function of time. Nothing happened after 50 seconds, so the results are truncated at that point. The experiments were carried out at two stress levels in the nearly linear region at 150°C.

For sample I strain recovery is substantially delayed by comparison with sample II and approximately 30% more strain is recovered (see Fig. 33).

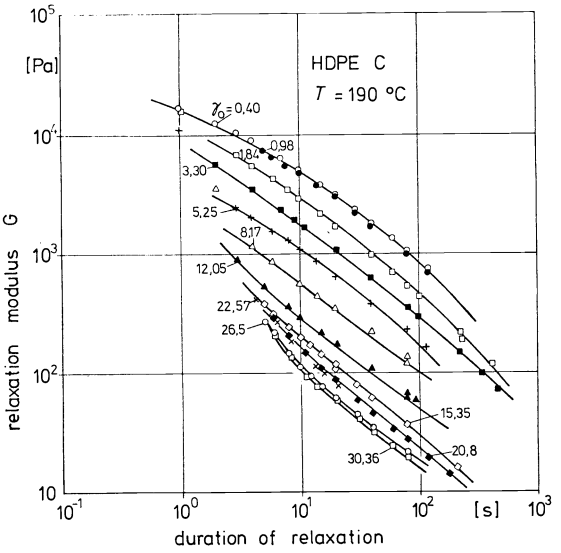

Fig. 32. Relaxation modulus of HDPE C measured in a step shear strain experiment (Hoechst). The parameter is the size of the shear strain γ_0. The relaxation modulus of HDPE Z is practically the same as the one of C.

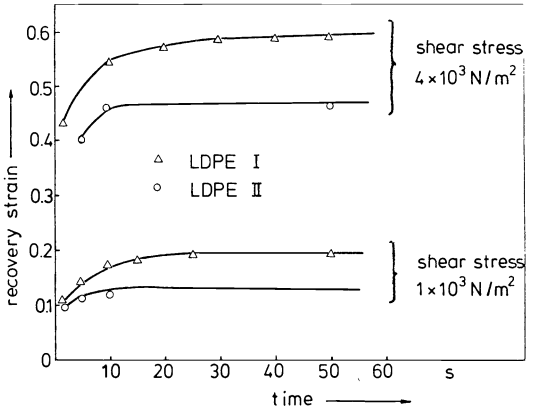

Fig. 33. Constrained recovery of LDPE samples after shear creep experiments at 150°C and 100 units of shears (ICI).

4.3.6. RHEOOPTICAL MEASUREMENTS, BIREFRINGENCE

TNO carried out experiments of measuring birefringence with a slit apparatus, described in (24). Tests were made at 150°C with a single slit die. The birefringence of the HDPE samples could not be measured properly because of the "streakiness" of the image. The streakiness might be due to lubricant migrating out of the polymer on to the wall surface. This disappeared very slowly with time, or could be made to disappear faster by an increase in temperature. The streakiness seemed to disappear faster with HDPE Z than with HDPE C. The images shown by the low-density polyethylenes were regular. The birefringence of LDPE I samples was about 40% higher than that of LDPE II at the same shear stress. Clearly, the materials differ either in their optical structures or in their relaxation rates of longitudinal gradients from the entrance region, or otherwise in their normal stress behavior. This result correlates with the pronounced differences in shear recovery.

4.3.7. PRESSURE DROP IN CONVERGING FLOW

The pressure drop was measured in three types of converging flow:

a. converging flow in a tapered tube (ICI). The diameter is reduced from 5 mm to 1 mm over a distance of 25.4 mm. The pressure transducer is situated at the entrance of the tube (barrel of 22 mm diameter).

b. flow through an orifice (die of zero length, L/D ≃ 0).
diameter of barrel: 9.55 mm
diameter of die: 1 mm (ME)
2 mm (ICI)
The pressure transducer is situated in the barrel at the capillary inlet.

c. entrance flow into capillaries. The pressure drop in capillaries of different L/D but of the same diameter is measured repeatedly at the same flow rate. The Bagley plot, p over L/D, allows for separating the entrance pressure correction p_c. The pressure transducer is situated in the barrel at the entrance of the die (or further upstream away from the entrance).

Data on LDPE

Sample I in converging flow requires a larger pressure drop than sample II. The largest differences occur in the pressure correction of the Bagley plot (see Figs. 34-36).

The difference between the two samples in converging flow was confirmed during constrained convergence in a tapered die (ICI). Here the difference is most clearly evidenced by the onset of non-laminar flow which occurs at a flow rate a factor of two higher for sample II than for sample I.

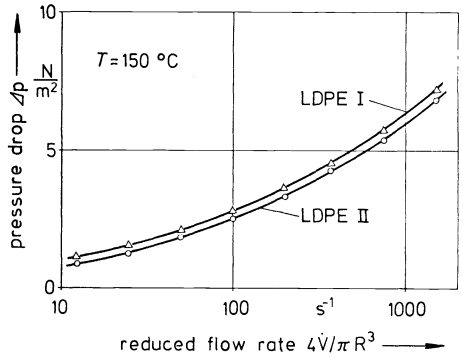

Fig. 34. Pressure drop in tapered tube versus reduced flow rate, with radius of reference R_o = 1 mm (ICI).

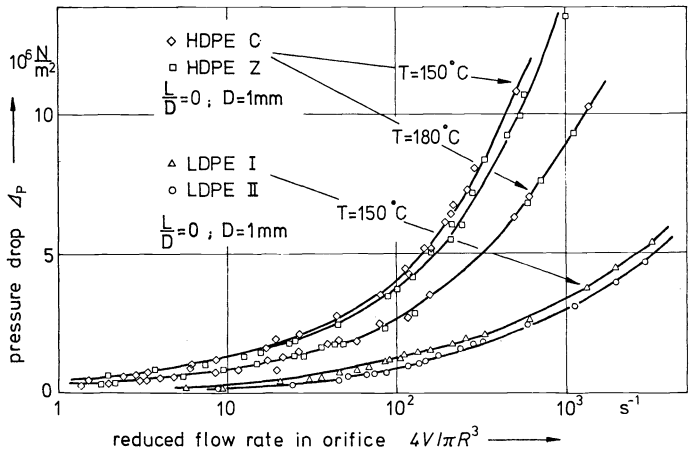

Fig. 35. Pressure drop for flow through an orifice (die of zero length, L/D = 0) (ME).

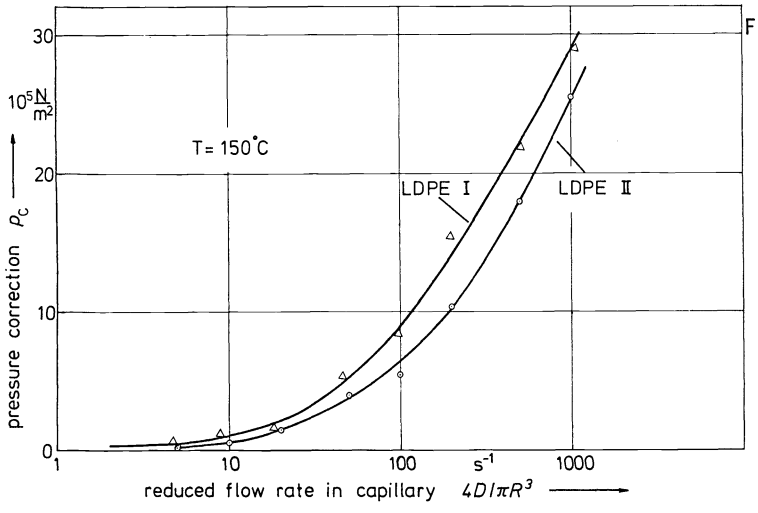

Fig. 36. Pressure correction p_c of Bagley plot versus reduced flow rate in capillary (BASF).

The pressure drop in orifice flow is about 30% higher for sample I. BASF reports significant differences in the entrance pressure correction (Bagley plot) for the two samples I and II (see Fig. 36). In the TNO experiments the entrance pressure correction is about the same for both samples only at the lowest temperature, T = 115°C, p_c is slightly higher for sample II than for sample I. The data measured at 150°C are compared in Table 12; note that the die geometries were very different in the two laboratories and hence the numbers are of different magnitude, but they can be used for a qualitative correlation.

TABLE 12: Pressure correction of LDPE samples as function of apparent wall shear rates (TNO, BASF).

$\dot{\gamma}_a[s^{-1}]$	LDPE I $p_c[10^5$ Pa]		LDPE II $p_c[10^5$ Pa]	
	115°C, TNO	150°C, BASF	115°C, TNO	150°C BASF
0.5	-	-	-	-
1	10	-	-	-
5	16	0.5	-	0.3
10	19	1.1	20	0.6
50	31	5.5	37	4
100	33	8.8	45	5.5

Data on HDPE

The pressure drop for flow through an orifice is the same for the two samples at 180°C. At 150°C sample C shows a larger pressure drop than sample Z (see Fig. 35).

3.4.8. EXTRUDATE SWELL

Sample I possesses a higher extrudate swell than sample II (Figs. 37-39). The two HDPE samples show the same amount of swell (Figs. 40, 41).

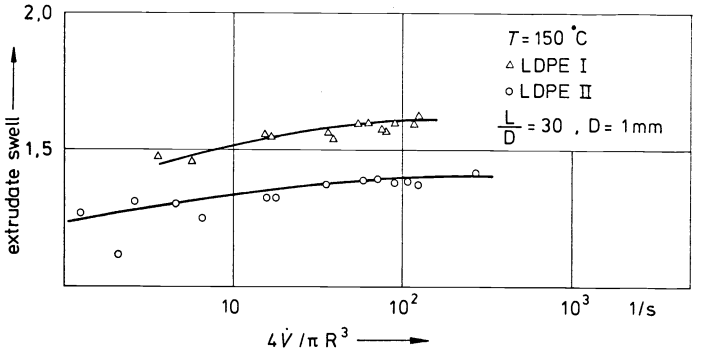

Fig. 37. Extrudate swell of LDPE samples as a function of flow rate, L/D = 30 (ME).

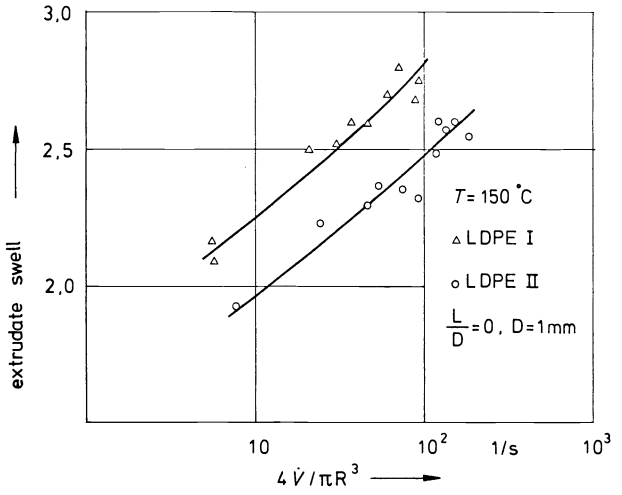

Fig. 38. Extrudate swell of LDPE samples as a function of flow rate, L/D = 0 (ME).

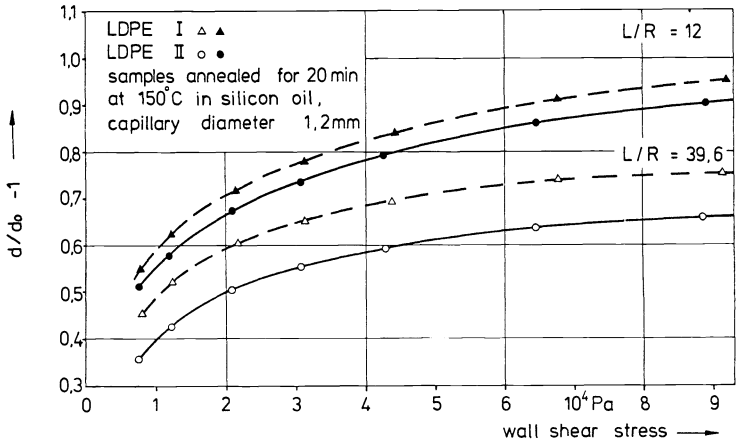

Fig. 39. Extrudate swell of LDPE samples as a function of wall shear stress, extrusion temperature T = 150°C (BASF).

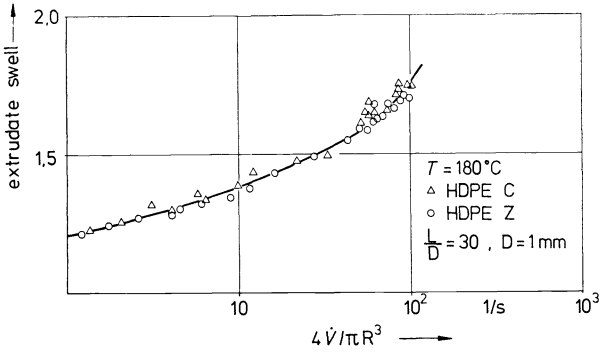

Fig. 40. Extrudate swell of HDPE samples as a function of flow rate, L/D = 30 (ME).

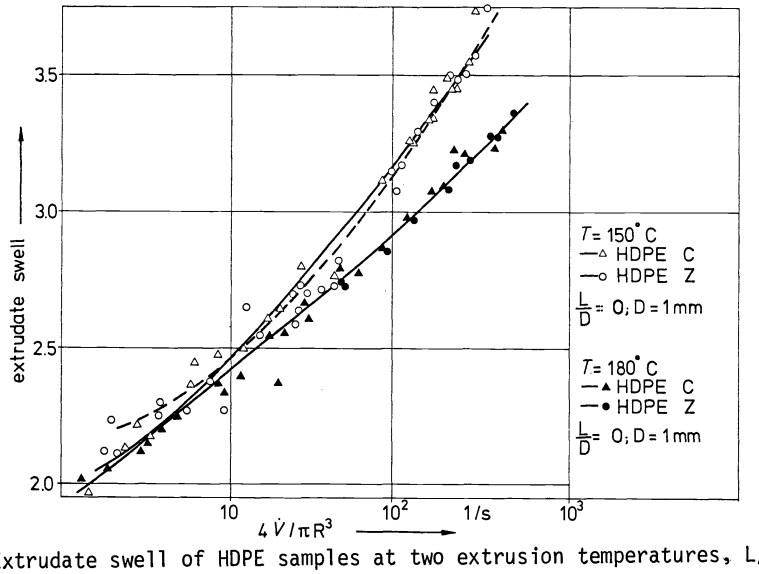

Fig. 41. Extrudate swell of HDPE samples at two extrusion temperatures, L/D = 0 (ME).

4.4. PROPERTIES IN UNIAXIAL EXTENSION

4.4.1. CREEP, RECOVERABLE STRAIN, AND STEADY STATE EXTENSIONAL VISCOSITY

The elongational properties were measured by means of a tensile creep apparatus (BASF, Hoechst). The cylindrically shaped sample was stretched at a constant stress and the resulting strain was recorded as a function of time. After unloading the sample the recoverable portion of the elongation can directly be measured at any state of deformation. The samples

were prepared by extruding the molten granules through the capillary of a viscometer at a temperature of 150°C. Afterwards they were annealed in a silicon oil bath for 20 min at 150°C in order to get entirely relaxed samples.

a) Creep curves

In Figs. 42 and 43 the total strain ε, the recoverable strain ε_r, and the viscous strain ε_v at a tensile stress of $\sigma = 5.10^3$ Pa are plotted as a function of time for the LDPE sample. Each symbol of the creep curve marks a separate experiment. After some time steady flow is reached, where the strain rate does not change any longer with time and the recoverable strain is constant. The total strain in creep and the viscous strain are much larger for LDPE I, while the recoverable strain is only slightly higher, see also Fig. 48.

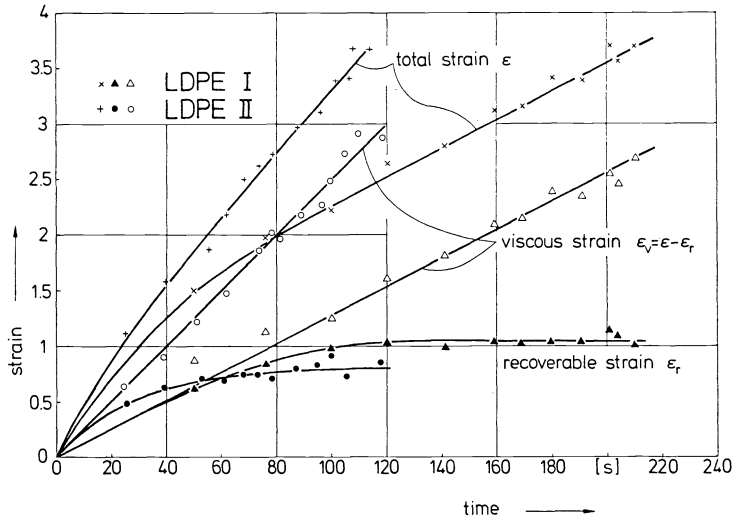

Fig. 42. Creep experiment with LDPE I and II; recoverable and viscous strain contributions in uniaxial extension (BASF), T = 120°C.

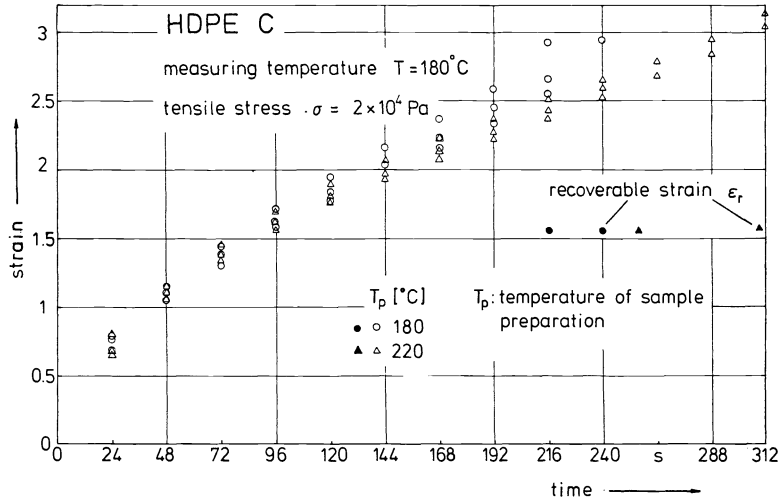

Fig. 43. Creep experiment with HDPE C; strain and recoverable strain as a function of time. The strain depends on the temperature of sample preparation (BASF), T = 180°C, tensile stress $\sigma = 2 \times 10^4$ Pa.

The creep curves of the HDPE samples are shown in Figs. 43-45. The strain of sample Z is significantly larger than the strain of sample C. The recoverable strain ε_r is about the same for both samples. The importance of sample preparation before rheological tests is shown in Figs. 43 and 44. The samples prepared at 220°C exhibit larger tensile stresses, possibly due to some cross linking during sample preparation.

b) Steady extensional viscosity

In the steady uniaxial extensional flow the viscosity is defined as the ratio of the tensile stress σ and the rate of extension $\dot{\varepsilon}$ (measured after constant values of σ and $\dot{\varepsilon}$ were reached).

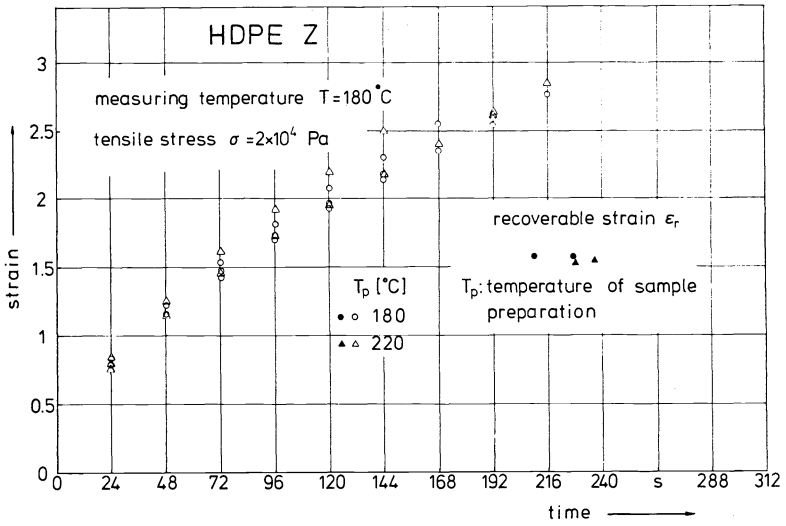

Fig. 44. Creep experiment with HDPE Z; strain and recoverable strain as a function of time. The strain depends on the temperature of sample preparation (BASF).

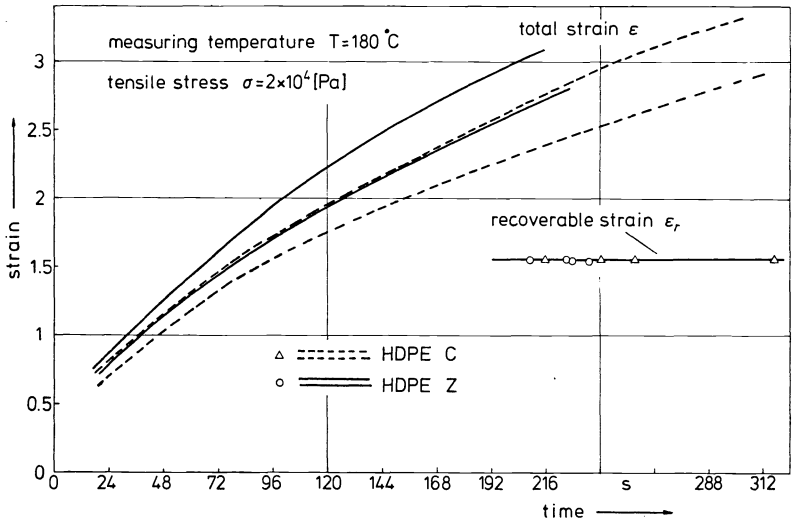

Fig. 45. Creep experiment with HDPE samples; strain as a function of time and recoverable strain. Comparison of data (BASF), T = 180°C, tensile stress $\sigma = 2 \times 10^4$ Pa. The spread of the data is due to the temperature of sample preparation (T_p = 180 and 220°C).

Data on LDPE

The extensional viscosity as a function of the applied tensile stress for both samples is plotted in Fig. 46. The viscosity increases with growing stress up to a maximum and falls down again. At small stresses the viscosity approaches the value $3\,\eta_0$. The viscosity functions of the two samples are nearly parallel to each other. Whereas the zero shear viscosities differ by about 25%, a factor of two is reached between the elongational viscosities at stresses higher than about 5×10^3 Pa. In a stress region where the viscosity functions in shear are indistinguishable, the elongational viscosities show a distinct difference which is expected to be reflected in the film blowing process.

Data on HDPE

The extensional viscosity of the HDPE samples was measured in a tensile creep experiment (Hoechst, BASF) and indirectly by an experiment involving orifice flow as proposed by Cogswell (25). The data are compared in Fig. 47.

c) Steady-state recoverable strain

In Fig. 48 the recoverable strain $\varepsilon_{r,s}$ in the stead-state as determined from retardation experiments is plotted as a function of tensile stress. For both samples $\varepsilon_{r,s}$ increases with stress (of the preceding creep experiment) and approaches a constant value which probably lies between 1.8 and 2.0. LDPE I shows a slightly higher recoverable strain than LDPE II.

The recoverable strain curves for both HDPE samples are not distinguishable from each other, see Fig. 49.

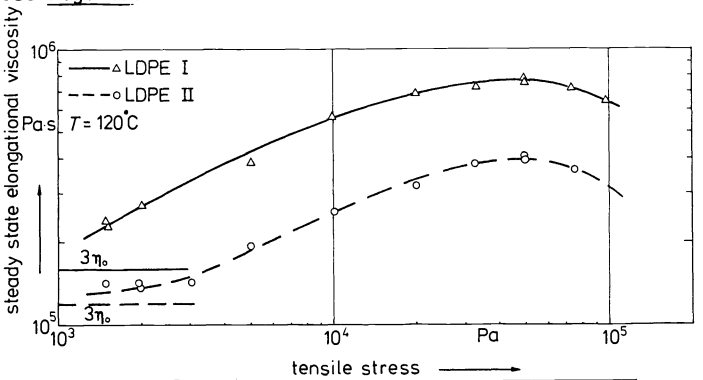

Fig. 46. Viscosity of LDPE samples in steady uniaxial extensional flow (BASF).

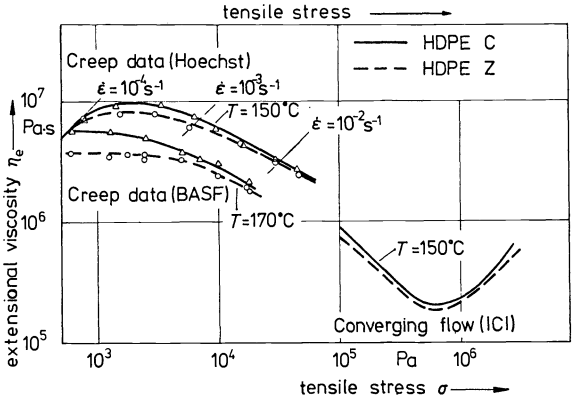

Fig. 47. Viscosity of HDPE samples in uniaxial extensional creep experiment with data from converging die flow.

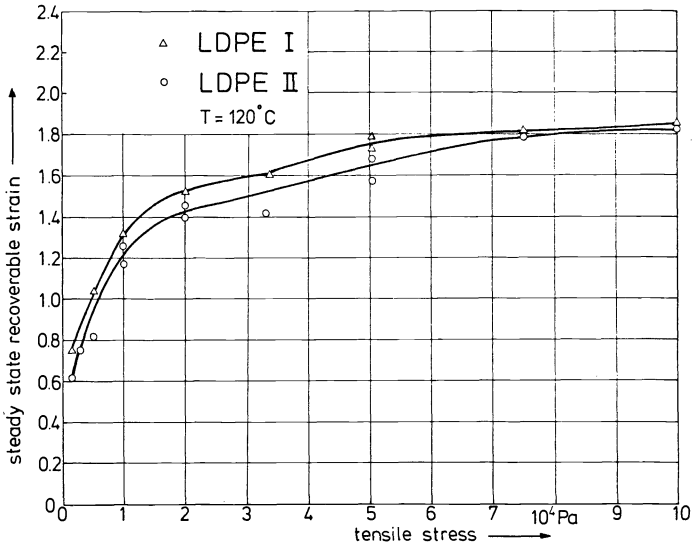

Fig. 48. Free recovery of LDPE samples after steady uniaxial extensional flow (BASF).

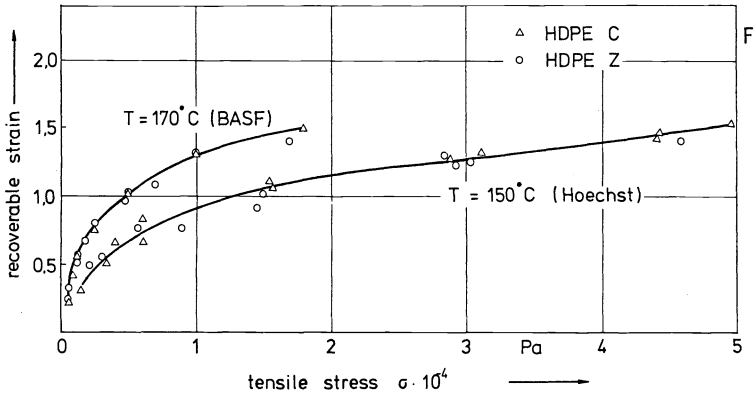

Fig. 49. Free recovery of HDPE samples after steady uniaxial extensional flow $\varepsilon = 3.5$ at BASF and $\varepsilon = 2.2$ at HOECHST.

4.4.2. TECHNICAL TENSILE TEST

In the tensile test a polymer is extruded vertically downward out of a die of circular cross section. In a distance L from the die exit, a stretching device pulls the extrudate with a take-up speed which is higher than the speed of the extrudate at the exit of the die. The tensile test is not a physically well defined test, mainly because 1) the temperatures are not uniform, 2) the rate of extension changes along the path of a polymer element, and 3) the upstream deformation history is determined by inhomogeneous shear. The results of the test, however, seem to be very valuable for comparing materials. Two similar types of tensile testers were used:

"Rheotens," developed by Meissner (26), manufactured by Fa. Gottfert,
"Melt Tension Tester," manufactured by Toyo Seiki Seisaku-sho LTD.

Three laboratories performed tests on the samples. The testing conditions are listed in Table 13. A small diameter of the extrudate and a long distance L favorize the cooling in the test section. The point of break of the filament is of special interest: The maximum force F_{max} represents the "melt strength," and the maximum drawdown ratio which is the ratio of the drawdown speed at break to the calculated die exit velocity, characterizes the "extensibility" of the melt.

TABLE 13. Comparison of experimental conditions of tensile test.

Laboratory	TNO	ME	ETH
Manufacturer	Gottfert	Seiki	Gottfert
Capillary diameter (mm)	2.03	1	2
length (mm)	0	8	30
Flow rate (mm^3/s)	33.7	23.8	
Velocity at exit (mm/s)	3.25	3.33	
Distance L from die exit to pulley (mm)	163	300	100 for LDPE 50 for HDPE

Data on LDPE

Sample I requires a larger tensile force than sample II at the same experimental conditions: Same temperature, same extension. Sample I breaks at smaller extension than sample II. Due to this smaller extension, the tensile stress at breakage is smaller in sample I than in sample II, even if at the same extension sample I requires the larger tensile stress. The data at break are compared in Table 14.

TABLE 14: Comparison of tensile test data at breakage for low density PE samples I and II.
*)no filament break within speed range of tensile tester.

Material	Sample I			Sample II		
laboratory	TNO	ETH	ME	TNO	ETH	ME
T = 120°C						
output rate $\dot{m}$ (g/min)						
take up velocity v_1 (mm/s)	267±10			421±23		
draw down ratio $V_b = v_1/v_o$	25.8			40.5		
extension at break ln V_b	3.25±0.05			3.70±0.06		
force at breakage F_b(N)	0.28±0.01			0.22±0.01		
diameter of filament at point of breakage d_b(mm)						
tensile stress at breakage $\sigma_b = 4\,F_b/\pi d_b^2$ ($10^5 N/m^2$)				27±1		
T = 150°C						
$\dot{m}$ (g/min)		7.9±0.3	13.1±0.3		7.9±0.5	13.1±0.3
v_1 (mm/s)	138±4			261±7		
$V_b = v_1/v_o$	13.2	13.3	11.6	129	25	14.3	12.6	262
ln V_b	2.58±0.03	2.59	2.45	4.86	3.22±0.03	2.66	2.53	5.57
F_b (N)	0.14±0.01	0.226	0.263	0.0299	0.085±0.01	0.18	0.223	0.0196
d_b (mm)								
$\sigma_b = 4\,F_b/\pi d_b^2$ ($10^5 N/m^2$)	6±0.5			7±0.5		
T = 180°C						
$\dot{m}$ (g/min)		7.3±0.3	11.3±0.3		7.3-0.3	11.3±0.3
v_1 (mm/s)						
$V_b = v_1/v_o$		16.3	14.5	170	19.5	*)	262
ln V_b		2.79	2.67	5.14	2.97	*)	5.57
F_b (N)		0.157	0.197	0.0172	0.107	*)	0.0102
d_b (mm)							
$\sigma_b = 4\,F_b/\pi d_b^2$ ($10^5 N/m^2$)							

The differences between the two samples are most pronounced in the experiment at low flow rate and a long distance between die and take-up roll, i.e., for long residence times in the stretching section (see Fig. 50).

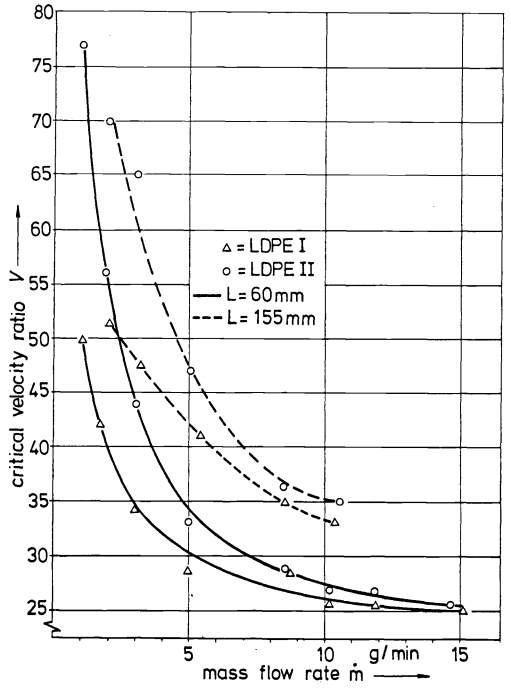

Fig. 50. Tensile test; critical velocity ratio (at which the thread breaks) as a function of mass flow rate and of distance between die exit and takeup roll (ETH).

Sample II shows weak draw resonance at 120°C and strong draw resonance at 150°C while sample I does not (reported by TNO). The filaments all broke near the gear wheels.

The pronounced difference in extensional behavior is also demonstrated by ICI experiments, when hanging weights on the extrudate (constant force extension). The draw ratio at break was found to be about four times higher for sample II.

Data on HDPE

The data at break are compared in Table 15. Due to significant differences in experimental conditions, one cannot expect the numbers to be very close. The extension at breakage is about the same for the two materials (ME, ETH) or it is somewhat smaller for HDPE C (TNO). Forces at break are about the same (TNO) or slightly higher for C (ME, ETH). Both materials show draw resonance (TNO). The test seems to be more sensitive at lower temperature.

4.5. CONCLUSIONS OF RHEOLOGICAL TESTS

The rheological behavior of the samples within each pair is found to be different. The difference, however, depends on the type of rheological experiment. The LDPE samples cannot be distinguished in shear flow at high shear rates; differences become evident in shear flow at medium and low shear rates and in extension at low rates (linear viscoelastic region); most pronounced are the differences in uniaxial extension at high rates. The HDPE samples are indistinguishable in most of the rheological tests, but pronounced differences appear in uniaxial extension.

In shear, the viscous material functions (shear viscosity, loss modulus) are less sensitive than elastic material functions (storage modulus, recovery, first normal stress difference, birefringence). This is also true for information taken from technical material functions (melt flow index, pressure corrections for entrance flow into capillaries, extrudate swell). The pressure correction p_c for entrance effects in capillary flow seems to be sensitive to small differences between materials, especially at low temperature. At very low temperature, differences in crystallization behavior influence the capillary flow experiment.

Extrudate swell seems to be a very sensitive measure for distinguishing the LDPE-samples (larger swelling of sample I), but no differences could be detected between behavior of samples C and Z.

The technological tensile test (stretching of extrudate from capillaries) gives significantly different data between the samples. The data of different laboratories can only be compared quantitatively, when die geometry, flow rate, stretching length, and geometry of take

up wheels are the same in collaborating laboratories (which was not the case here).

TABLE 15: Comparison of tensile test data at breakage for high density PE samples C and Z.

Material	Sample C			Sample Z		
laboratory	TNO	ETH	ME	TNO	ETH	ME
T = 150°C						
output rate $\dot{m}$ (g/min)	47±3			79±2		
take up velocity v_1 (mm/s)	4.57			7.61		
draw down ratio $V_b=v_1/v_o$	1.52±0.07			2.03±0.02		
extension at break ln V_b	0.61±0.02			0.65±0.01		
force at breakage F_b(N)						
diameter of filament at point of breakage d_b(mm)						
tensile stress at breakage $\sigma_b=4\ F_b/\pi d_b^2$ (10^5N/m^2)						
T = 180°C						
$\dot{m}$(g/min)		5.1±0.2	15.2±0.4		5.1±0.2	15.2±0.4
v_1(mm/s)	158±8			189±11		
$V_b=v_1/v_o$	15.2	7.5	6.4	89	18.4	6.6	7.5	90
ln V_b	2.72±0.07	2.01	1.86	4.49	2.91±0.1	1.89	2.01	4.5
F_b (N)	0.28±0.01	0.553	1.050	0.069	0.28±0.01	0.527	1.000	0 066
d_b (mm)								
$\sigma_b=4\ F_b/\pi d_b^2$ (10^5N/m^2)								
T = 210°C						
$\dot{m}$(g/min)		5.1±0.1	14.2		5.1±0.1	22.2
v_1(mm/s)						
V_b		7.2	5.3		7.5	5.7
ln V_b		1.97	1.67		2.01	1.74
F_b (N)		0.42	0.733		0.387	0.88
d_b (mm)						
$\sigma_b=4\ F_b/\pi d_b^2$ (10^5N/m^2)						

5. CONCLUSIONS

The two pairs of polyethylenes show very pronounced differences in film blowing. LDPE I and HDPE C are much more difficult to draw into a thin film than LDPE II and HDPE Z. The difference between the samples shows up in some of the rheological tests, but not in all of them. Besides rheology, the crystallization behavior seems to be very influential.

The two LDPE samples are similar in molecular weight distribution and in branching. LDPE I has a slightly higher average molecular weight due to a heavier tail of high molecular weight molecules. The thinnest films blown in steady operation were of thickness 8 μm for the LDPE I and 4 μm for LDPE II. The bubble shape (at same A and V) is considerably different for the two samples. Differences in drawing behavior are amplified by the bubble cooling process which heavily depends on the distribution of wall thickness in the bubble. Sample I adjusts at much higher freeze lines than sample II, when the operating conditions of the cooling system are set the same. The internal pressure is about the same for both LDPE samples, the axial force is significantly higher for LDPE I. The orientation, as measured by the retraction ratio of the film, is slightly higher in films blown from LDPE I.

The LDPE samples exhibit larger differences in the linear viscoelastic behavior. They are most pronounced in experiments which are determined by larger relaxation times: Measurement of zero viscosity and of first normal stress coefficient, measurement of complex shear modulus at low frequency, extrusion at low rate. LDPE I has a higher zero viscosity, higher shear stress and higher normal stress difference in stress growth at low rates, and higher complex modulus.

The two LDPE samples show minor differences in entrance pressure correction at 120°C. The corrections are 10% greater for LDPE I than for LDPE II, but at 115°C the reverse is the case. Extrudate swelling is larger with LDPE I.

The relaxation behavior shows larger differences between the samples in the sense that at a given shear rate the relaxation is always farther for sample II than for sample I. LDPE I has a broader spectrum of relaxation times, probably due to tails of high molecular weights, than LDPE II. Moreover the relaxation spectrum of sample I is more shear sensitive than that of sample II as shown by faster increase in relaxation speed by increasing shear rate.

LDPE I has a higher tensile viscosity. In tensile tests, it has a lower extensibility and a lower "melt strength" than sample II; sample II shows draw resonance, sample I does not.

Sample I starts to crystallize at a higher shear rate than sample II. The spherulitic radii are bigger for sample II.

The two HDPE samples are taken from the same powder lot. They only differ by the processing aid, calcium stearate or zinc stearate. HDPE C can be drawn into a film of 4 μm thickness, while HDPE Z can be drawn much further, 1.5 μm. The bubble shape and the temperature distribution in the bubble differ considerably for the two HDPE samples. These differences, however, do not appear in the shrinkage of the films.

Significant differences were found in the mechanical strength. The impact strength was much higher for films from sample Z, especially when blown in the bubble with a long stem.

The HDPE samples show no significant differences in viscosity functions, stress buildup, relaxation properties, extrudate swelling. Sample C has a higher extensional viscosity than sample Z. In tensile tests, HDPE C shows the same or a smaller extension at break (depending on the setup); both materials show draw resonance. The "melt strength" is about the same for the two HDPE samples.

Dynamic calorimetric behavior does not show a difference, but small differences could be found in the isothermal crystallization behavior.

For both pairs the sample with the lowest tensile stress in extensional flow can be drawn into the thinnest film. This is in agreement with findings of the preceding study (1).

NOMENCLATURE

A	-	blow up ratio in film blowing d_f/d_o
d,D	m	diameter
F	N	force
G'	Pa	storage modulus
G''	Pa	loss modulus
h	m	gap width
L	m	capillary length
p	Pa	pressure
p_c	Pa	pressure correction
r,R	m	capillary radius, bubble radius
s	m	film thickness
T	$^oC, ^oK$	temperature
v	m/s	velocity
V	-	velocity ratio in film blowing, v_f/v_o
$\dot{V}$	m^3/s	volume flow rate
z	m	distance from die exit (film blowing)
γ	-	shear strain
$\dot{\gamma}$	s^{-1}	shear rate
ε	-	extensional strain
$\dot{\varepsilon}$	s^{-1}	rate of extension
ε_v	-	recoverable strain, $\varepsilon-\varepsilon_v$
ε^v	-	viscous strain, $\varepsilon-\varepsilon_r$
η	Pa s	viscosity of steady shear flow
η_o	Pa s	zero shear viscosity
λ	s	relaxation time
μ_s	Pa s	steady extensional viscosity
σ	Pa	tensile stress in uniaxial extension
τ	Pa	shear stress in shear flow

INDICES

f	measured on film
o	at die exit (film blowing experiments)
r	recoverable
s	steady state

REFERENCES

1. J. Meissner, Pure and Appl. Chem. 42, 553 (1975).
2. P. K. Agarwal and D. J. Plazek, J Appl. Polym. Sci. 21, 3251 (1977).
3. J. H. Magill and S. Peddada, J. Polym. Sci.: Polym. Phys. Ed. 17, 1947 (1979).
4. P. L. Clegg and N. D. Huck, Plastics 26, 107 (1961).
5. J. R. A. Pearson and C. J. S. Petrie, Plastics Polymers 38, 85 (1970), J. Fluid Mech., 42, 609 (1970).
6. R. Farber and J. Dealy, Polym. Eng. Sci. 14, 435 (1974).
7. B. Poltersdorf, M. M. Balashov and Y. S. S. Borodkin, Plaste Kautschuk 21, 929 (1974).
8. C. D. Han and J. Y. Park, J Appl. Polym. Sci. 19, 3257 (1975); 19, 3277 (1975); 19, 3291 1975).
9. M. H. Wagner, Rheol. Acta, 15,40 (1976).
10. T. Yamaguchi, T. Yanagava and H. Kimura, Sen'i Gakkaishi 32, 470 (1976).
11. C. D. Han and R. Shetty, Ind. Eng. Chem. Fund. 16, 49 (1977).
12. W. Ast, Kunststoffe 63, 427 (1973).
13. M. Swerdlow, F. N. Cogswell, and N. Krul, Plastics Rubber Proc. 11 (1980).
14. M. E. A. Cudby and A. Bunn, Polymer 17, 345 (1976).
15. J. C. Randall, J. Polym. Sci.: Polym. Phys. Ed. 11, 275 (1973).
16. D. E. Dorman, E. P. Otocka, and F. A. Bovey, Macromolecules 5, 574 (1972).
17. N. R. Wilson, M. E. Bentley, and B. T. Morgan, SPEJ 26, 34 (1970).
18. J. S. Schaul, M. J. Hannon, and K. F. Wissbrun, Trans. Soc. Rheol. 19a, 351 (1975).
19. H. H. Winter and E. Fischer, Polym. Eng. Sci. 21, 366 (1981).
20. K. H. Illers, Europ. Polym. J. 10, 911 (1974).
21. A. K. van der Vegt and P. P. A. Smit, SCI Monograph 26, 313 (1967).
22. E. Uhland, Rheol. Acta. 18, 1 (1979).
23. H. M. Laun, Rheol. Acta. 17, 1 (1978).
24. J. L. S Wales, Thesis, Delft, (1976).
25. F. N. Cogswell, Polym. Eng. and Sci. 12, 64 (1972).
26. J. Meissner, Trans. Soc. Rheol. 16, 405 (1972).